

FEA Modelling of Weld-deposition based Additive Manufacturing for the Residual Stress Prediction

Maddu Naveen Kumar

A Dissertation Submitted to
Indian Institute of Technology Hyderabad
In Partial Fulfillment of the Requirements for
The Degree of Master of Technology



भारतीय प्रौद्योगिकी संस्थान हैदराबाद
Indian Institute of Technology Hyderabad

Department of Mechanical & Aerospace Engineering

June, 2014

Declaration

I declare that this written submission represents my ideas in my own words, and where others' ideas or words have been included, I have adequately cited and referenced the original sources. I also declare that I have adhered to all principles of academic honesty and integrity and have not misrepresented or fabricated or falsified any idea/data/fact/source in my submission. I understand that any violation of the above will be a cause for the disciplinary action by the Institute and can also evoke penal action from the sources that have thus not been properly cited, or from whom proper permission has not been taken when needed.

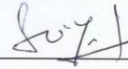


Maddu Naveen Kumar

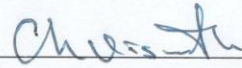
ME12M1014

Approval Sheet

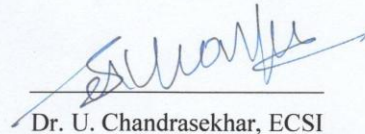
This thesis entitled “FEA Modelling of Weld-deposition based Additive Manufacturing for Residual Stress Prediction” by Maddu Naveen Kumar is approved for the degree of Master of Technology from IIT Hyderabad.



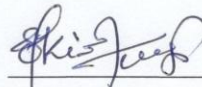
Dr. S. Suryakumar, IIT Hyderabad
Adviser



Dr. Viswanath Chinthapenta, IIT Hyderabad
Internal Examiner



Dr. U. Chandrasekhar, ECSI
External Examiner



Dr. P. A. Lakshmi Narayana, IIT Hyderabad
Chairman

Acknowledgements

I would like to express my sincere thanks to my adviser **Dr. S. Suryakumar** for his constant support throughout my thesis work. His logical way of thinking and enthusiastic support motivated me a lot to do this project. The discussions that I had weekly with him were a major source of learning and improving my knowledge. Without his guidance and persistent help this thesis would not have been possible.

I owe my most sincere gratitude to **Dr. Viswanath Chinthapenta** who helped me to untangle the typical knots in coding part of my thesis.

I am grateful to **Somashekara** for sharing of knowledge and helping me a lot in my thesis work. I would like to thank my friends **Himasekhar Sai** and **Syed Quadir** for their cooperation and generous help throughout my project. I would like to thank **Ramesh** for helping me in the manufacturing and metrology lab.

I would like to express my heartfelt thanks to all my classmates and friends for giving me the moral support.

Dedicated to

My beloved family

Abstract

Research in the development of additive manufacturing process employing direct metal deposition for the fabrication of fully functional parts and tooling has generated significant interest in the recent years. Three-dimensional welding is being investigated as an additive manufacturing technique for the production of real metallic parts using gas metal arc welding (GMAW) principles. The temperature field distribution during weld based rapid prototyping induces complex thermal stress evolutions and plays a big role in residual stress distributions.

The present work is to investigate the temperature field and thermal stress distributions in the multi-pass single-layer weld-deposition based additive manufacturing using twin wire welding. A three-dimensional finite element model with the temperature-dependent material properties and moving heat source is modelled for the same. A double ellipsoidal heat source model is applied to calculate the twin wire welding's temperature field is used. The filler metal deposition is taken into account by implementing the birth-and-death functionality for the finite elements. The temperature distribution pattern and magnitude is subsequently obtained. This result is then used for estimation of residual stress and distortion due to the twin wire welding.

The FEA model was then validated with the help of the experiment results. Using XRD machine the residual stress distributions of depositing component are estimated. A good match is found between both the FEA Simulation and experimental results

Content

Declaration	ii
Approval Sheet	iii
Acknowledgement	iv
Abstract	vi
Nomenclature	ix
List of Figures	x
Chapter 1: Introduction	
1.1 Additive Manufacturing	1
1.2 Classification of metallic AM Process	2
1.2.1 Laminated Object Manufacturing	3
1.2.2 Powder Bed Technology	3
1.2.3 Deposition Technologies	4
1.3 Area Filling	6
1.4 Time twin Welding	7
1.4.1 Metal transfer in Time twin weld-deposition	8
1.4.2 Welding speed and deposition rate	9
1.5 Residual Stresses	9
1.6 Problem Definition	10
1.7 Organization of report	11
Chapter 2: Literature survey	
2.1 Study on numerical modelling of welding	12
2.2 Computational Welding Mechanics	12
2.3 Study on residual stresses developed during weld-deposition	13
2.4 Studies on temperature field and stress distributions during weld based additive manufacturing	16
2.5 Study on temperature field during Twin Wire welding	17

Chapter 3: Finite Element Modelling of Weld-deposition		
3.1	Introduction	18
3.2	Thermo-Mechanical Analysis of Welding	18
3.3	Governing Equations and Finite Element Evaluation	19
3.3.1	Thermal Analysis	19
3.3.2	Mechanical Analysis	19
3.4	Boundary Conditions	19
3.4.1	Thermal Boundary Conditions	19
3.4.2	Mechanical Boundary Conditions	20
3.5	Modelling of Heat Source	21
3.5.1	Heat source modelling of twin wire welding	23
3.5.2	Modification of heat source formula	24
3.6	Filler Material Addition	25
3.7	Material Properties	26
3.8	Application of Heat generation	27
3.9	ANSYS Analysis Procedure	28
3.9.1	Assumptions during Thermal and structural modelling in ANSYS	29
3.10	Simulation Results	30
Chapter 4: Experimental Validation		
4.1	Introduction	32
4.2	Experimental setup and procedure	32
4.2.1	Setup of depositing system	32
4.2.2	Power source	34
4.2.3	Design of fixture	34
4.2.4	Experimental procedure	36
4.2.5	Measurement of residual stresses	38
4.3	Comparison of experimental and simulation results	39
Chapter 5: Conclusions and Future Scope		42
References		44

Nomenclature

q- Heat flux

E- Modulus of elasticity

C- Distribution coefficient

t- Time

ρ - Density of material

c- Specific heat capacity of the material

k- Thermal conductivity

η - Arc efficiency

V- Voltage

I- Current

S- Weld torch speed

β – Arc deviation

h- Heat transfer coefficient

T- Temperature

ϵ_0 - Emissivity

σ_0 - Stefan–Boltzmann constant

List of Figures

1.1	Additive manufacturing process	2
1.2	Classification of additive manufacturing	2
1.3	Laminated object manufacturing	3
1.4	Powder bed technology (Selective Laser Sintering)	4
1.5	Schematic of welding based rapid prototyping	5
1.6	Different types of area filling methods	6
1.7	Different types of contour area filling methods	7
1.8	Functional principle of Time Twin Digital separate welding potential	8
1.9	Schematic representation of the metal transfer and welding-current time-curves for Twin wire	8
2.1	Different domains of CWM	13
3.1	Boundary condition for thermal analysis	20
3.2	Boundary conditions for structural analysis	21
3.3	Double ellipsoidal heat source model	22
3.4	Droplets transiting track of twin wire welding	23
3.5	The revolute diagrammatic sketch of double ellipsoid heat source model	24
3.6	Addition of filler material in simulation of welding operation	26
3.7 (a)	Thermal material properties for steel considered	26
3.7 (b)	Young's modulus and Poisson Ratio as function of temperature	26
3.8	Detailed sequentially coupled thermo-mechanical ANSYS analysis	28
3.9	Three-dimensional finite element model	29
3.10 (a)	Temperature distribution of 1 st pass when source is at middle	30
3.10 (b)	Temperature distribution of 4 th pass when source is at middle	31
3.10 (c)	Temperature distribution of 9 th pass when source is at middle	31
4.1	Simple drawing of welding set up and wire spool connecting with robot	33
4.2	Welding deposition system integrated with Robot machine	33
4.3	Complete welding system based on the power source Time Twin Digital 5000	34
4.4	AUTOCAD figure of Fixture	35

4.5	Figures of fixtures before and after the deposition	36
4.6	Experimental Setup of base plate and Deposition Sequence	37
4.7	X-Ray Diffraction residual stress measurement instrument	38
4.8	XRD Measurement of Residual stress axially and diagonally	39
4.9	Comparison between experimental and simulated residual stress axially	40
4.10	Comparison between experimental and simulated residual stress diagonally	41

Chapter 1

Introduction

1.1 Additive Manufacturing

Rapid Prototyping (RP) is an automatic process of manufacturing objects (parts, prototypes, tools and even assemblies) directly from their CAD models without any cutters, tools or fixtures specific to the object geometry. It is one of the fastest growing automated manufacturing technologies that have significantly impacted the length of time between initial concept and actual part fabrication. RP process begins by creating a solid model of the product using any CAD interface. The solid model geometry is sliced into layers and required deposition path for each layer is generated. This layer wise data is send to the deposition system to build the part layer by layer. To accommodate geometries with overhanging features the parts are embedded in a sacrificial supporting material during build. The process automation and subsequent shorter production time is the primary advantage of rapid prototyping over the traditional manufacturing processes.

Before arriving on the term additive manufacturing, it was referred using various terms like Rapid prototyping, Rapid Tooling, Rapid Manufacturing, Solid Freeform Fabrication, 3Dprinting, thanks to the latest ASTM standards on its terminology[1].

There are number of steps that are involved, ranging from creating a CAD file to realization of physical form as shown in figure 1.1. Simple products make use of Additive Manufacturing (AM) only, while complex and higher engineering parts adopts numerous stages and iterations during the development stage.

Various processes that are involved in the additive manufacturing process are

1. Development of CAD file
2. Conversion to STL format
3. Transferring file to machine
4. Changing machine settings

5. Building model
6. Removal process and cleaning
7. Post-processing of the part
8. Applications

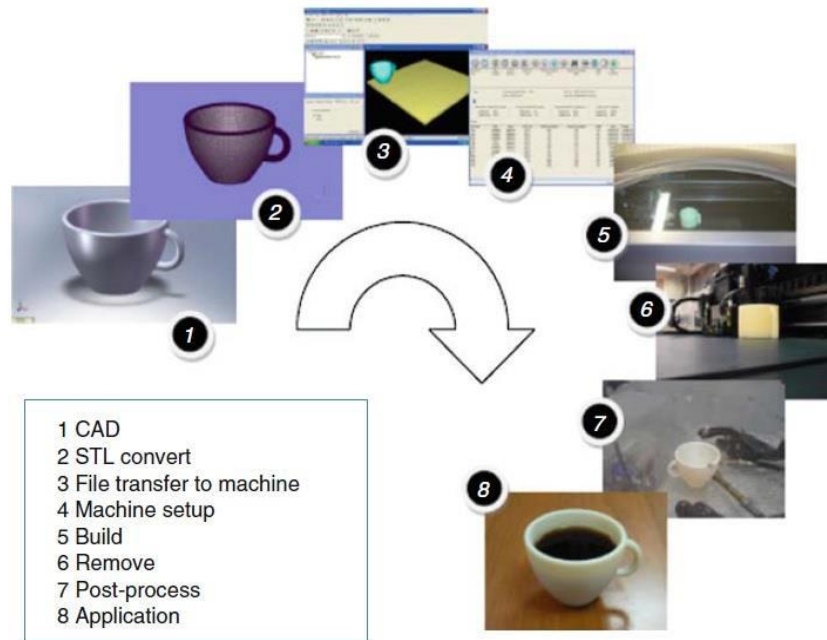


Figure 1.1: Additive manufacturing process

1.2 Classification of metallic AM Process

The additive manufacturing process can be classified into different types based on the technology and the type of raw materials used as shown in figure 1.2.

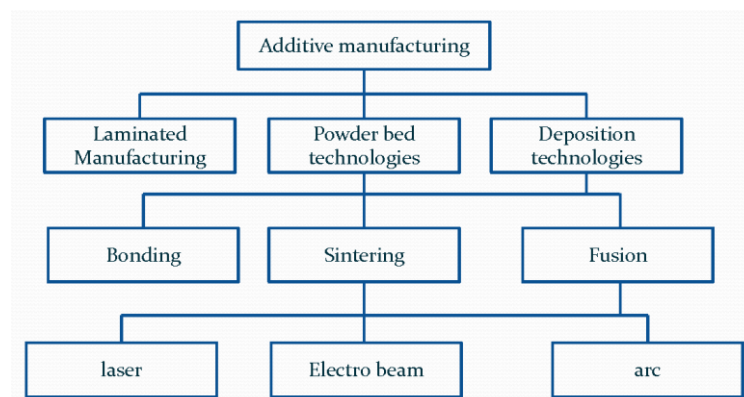


Figure 1.2: Classification of additive manufacturing

1.2.1 Laminated Object Manufacturing

The first commercialized sheet laminated process is sheet laminated object manufacturing (LOM) and is developed by Helisys Inc. (Cubic Technologies is now the successor organization of Helisys) In this process, paper is laminated in layer by layer fashion and cutting is done by laser or by sharpened blades as shown in figure 1.3. There are many laminated manufacturing techniques that build different materials and cutting techniques. This process is robust, flexible and valuable for many applications. And layered cross section can be manufactured quickly since trimming is required only in the boundary unlike other AM process. Laminated object manufacturing can be classified into further forms like 1) gluing or adhesive bonding, 2) thermal bonding processes 3) clamping, and 4) ultrasonic welding.

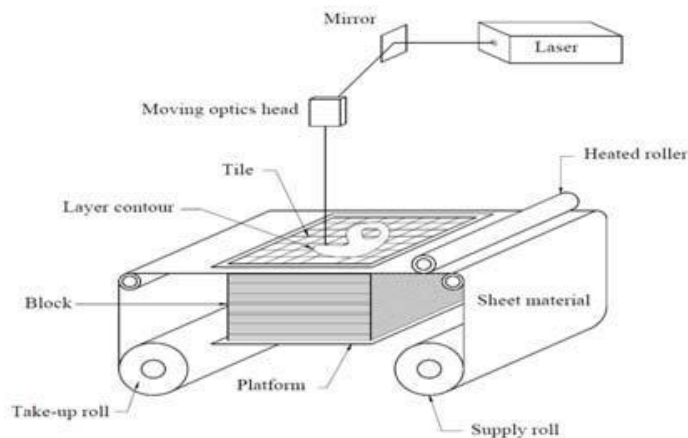


Figure 1.3: Laminated object manufacturing

1.2.2 Powder bed technology

It is one among the first commercialized AM product. Selective laser Sintering (SLS) which was developed at the University of Texas at Austin, USA, was the first to be commercialized. In the powder bed fusion process a layer of raw material in powdered form is spread over the platform, then the desired shape is obtained by creating a solid shape. Here, a separate support mechanism is not required since the unsolidified surface remains and acts as a support mechanism as shown in figure 1.4. Powder bed technology can be further classified into four different mechanisms[2]; Solid state sintering, chemically induced binding, liquid phase sintering and full melting.

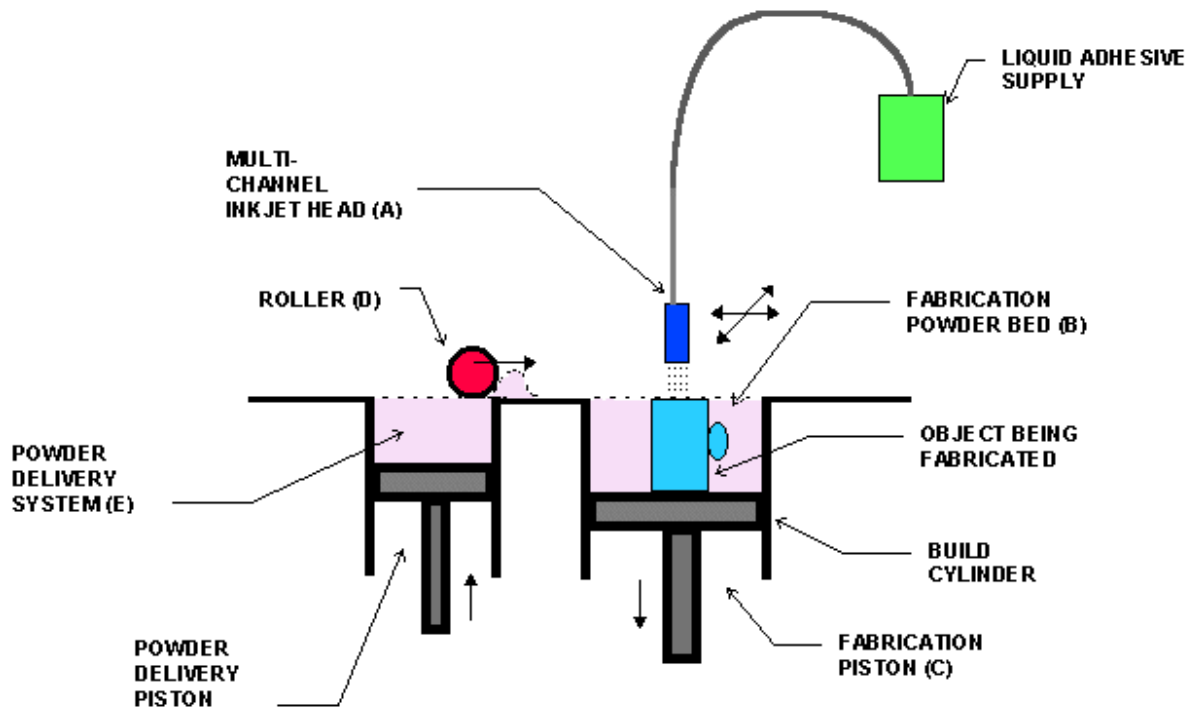


Figure 1.4: Powder bed technology (Selective Laser Sintering)

1.2.3 Deposition technologies : Weld Based Deposition

This category of additive manufacturing technique comprises of all those methods which use welding as a metal deposition process. A welding arc provides the heat to melt the wire, fed by a wire feeding system, while a CNC program developed using the CAD data is used to place the welding torch at required position for the deposition. This method is also referred to as 3D welding and is still in its experimental phase, as research is in progress to reduce the problem associated with weld base deposition like residual stresses, poor surface finish and deformations[3]. This method has the capability of producing form fit and functional parts. A major development is the Hybrid RP system which uses gas metal arc welding and CNC milling. 3D welding and milling is a novel freeform fabrication process and allows the fabrication of metallic prototypes by combined additive and subtractive techniques. Figure 1.5 shows the process principle of 3D welding and milling. First, a layer is built by depositing single beads side by side with bead offset. Depending on the welding parameters such as welding speed and welding power, the bead thickness varies. The distance between single beads is an important process parameter determining the overlapping of beads and thereby

the layer's surface quality. When deposited, the top surface of the layer is machined to a prescribed thickness for further deposition. Combining the deposition with subsequent face milling enables us to make appreciable changes in the layer thickness. This is, in fact, a unique feature of the process in that an adaptive slicing with variable layer thickness is enabled. When the sequence of deposition and face milling is finished, surface finishing is applied in the same setup to remove remaining stair steps on the surface. Any dimensional and geometrical inaccuracy resulting from the deposition can be completely compensated for by this surface finishing. It has been demonstrated that prototypes with simple geometries such as thin-walled and solid rectangular shapes can be built with this process. The deposition by gas metal arc welding is a cost effective method of metal deposition; however its beads are of lower quality than laser welding beads with respect to accuracy and surface quality. Since a post-processing step, e.g. surface machining is required for most of the parts built by direct deposition approaches, the relatively low accuracy and surface quality of arc-welded beads is acceptable. GMAW also offers a distinct technical advantage with regard to the possibility of vertical wire feeding; the welding result is independent from the change of the relative movement between the wire nozzle and x-y table.

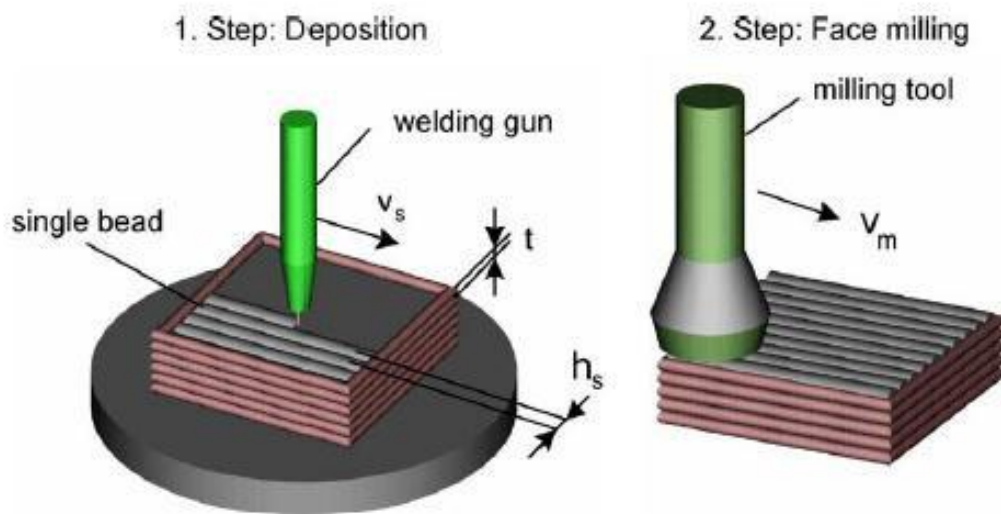


Figure 1.5: Schematic of welding based rapid prototyping

GMAW and GTAW are the two most commonly used method of metal deposition by 3D welding. The advantage of GMAW is the high rate of metal deposition and the ease of welding, on the other hand in GTAW the rate of deposition is relatively low but gives good surface finish since the wire feed rate is independent of welding current. Moreover the beads

can be partially or fully overlapped with no influence on arc stability. Due to reduce spatter in GTAW process, surface milling after each deposited layer is avoided, which increases the process speed.

1.3 Area Filling

In order to fill a layer using beam deposition, proper path planning is to be done for the weld torch to fill the area in the effective way. There are mainly two types of area filling paths Fig 1.6 [a, b]

- a) Direction-parallel area-filling
- b) Contour-parallel area-filling.

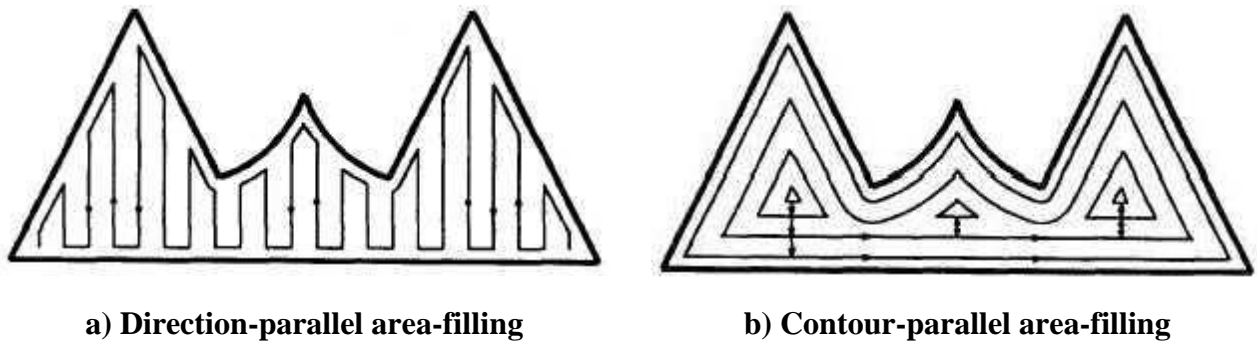
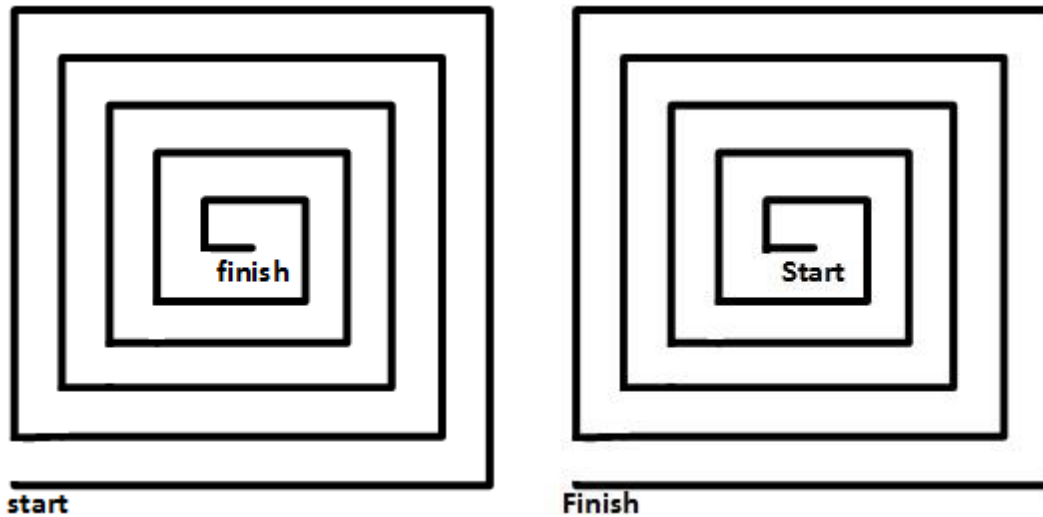


Figure 1.6: Different types of area filling methods[4]

Direction parallel filling is also known as raster filling while contour parallel is known as vector filling or spiral filling. The fundamental difference is that in the former the path starts from one end of the area and ends at the other parallel to any of the axis of the coordinated system, slowly filling in a zigzag manner, while in later the path is parallel to the perimeter. Directional parallel area filling can be further classified into in line area filling and zigzag area filling. Inline area filling is having unidirectional paths hence it is not continuous while in zigzag, filling takes place in both directions in a continuous path. Contour parallel area filling is of two types, outside- in contour and inside-out contour. In former the path starts from outside and fills towards inside and ends in the middle and later is just reverse of the same, i.e. first the centre is being filled then moving to the outside perimeter as shown in fig1.7.



(a) Outside-in contour filling

(b) Inside-out contour filling

Figure 1.7: Different types of contour area filling methods [5]

1.4 Time twin Welding

The Time Twin weld-deposition is two wires one process. With Time Twin, controllable digital power sources work totally independently with two separate filler wires in just one gas nozzle and in a common weld pool. This shortens the cycle times and increases the weld quality and productivity in high-performance welding. Arcs are selectively controllable and metal-transfer processes from both the wire electrodes can be timed to co-ordinate with one another (i.e. either synchronized or pulsed-displaced). The arc blow effect in pulsed arc and low-spatter metal transfer is minimal with almost constant droplet size. The power-source characteristic can readily be adjusted to the base metal and filler metal, and to the shielding gas. Mainly functioning of the time twin electrodes are welded in a single weld-pool, under the shielding gas atmosphere. The wire is fed by two separate wire feeders; these wire feeders in turns are powered by two power sources, each of which is independent of the other two synchronized power sources. The two wire electrodes are brought together in the welding torch in such a way that there are two separate welding potentials. Figure 1.8 illustrates functional principle of Time Twin Digital separate welding potential.

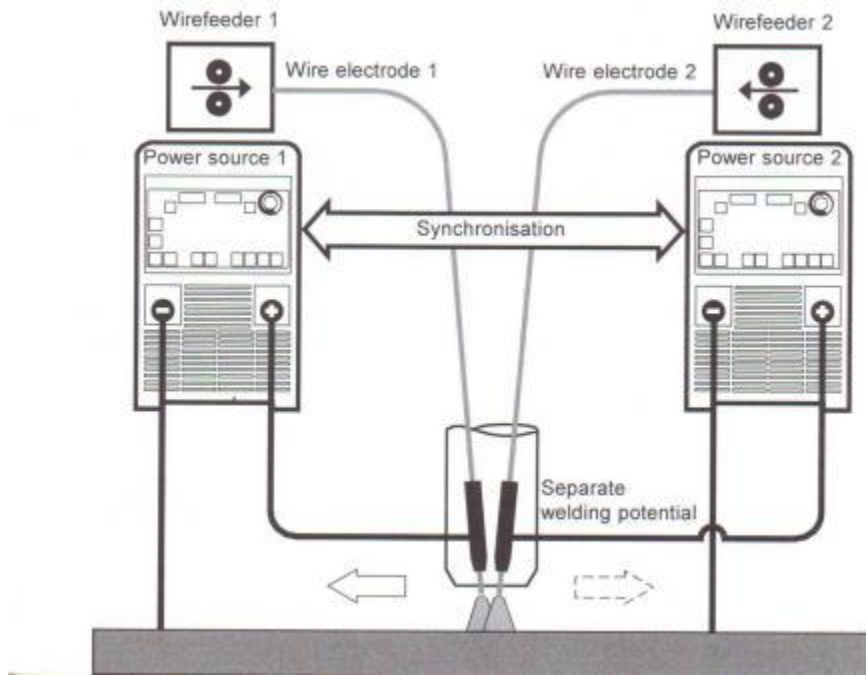
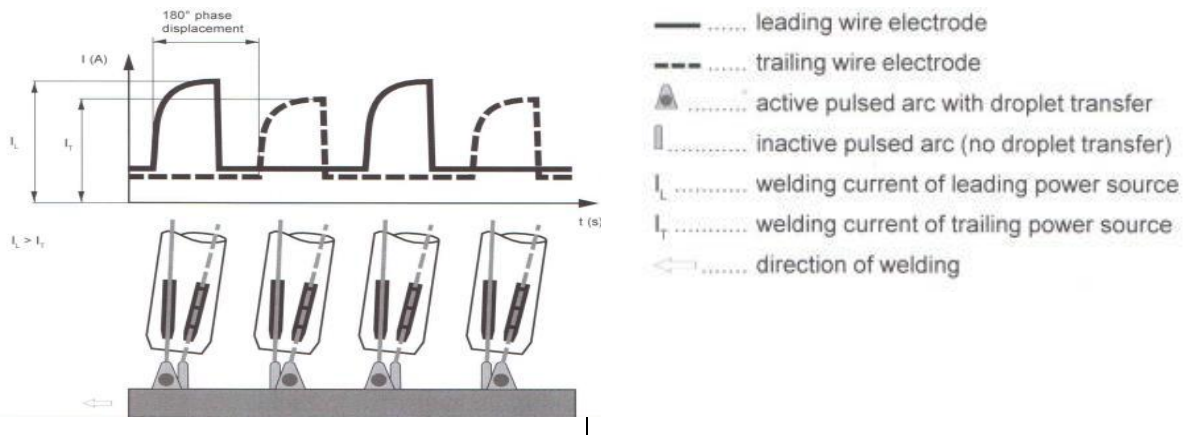
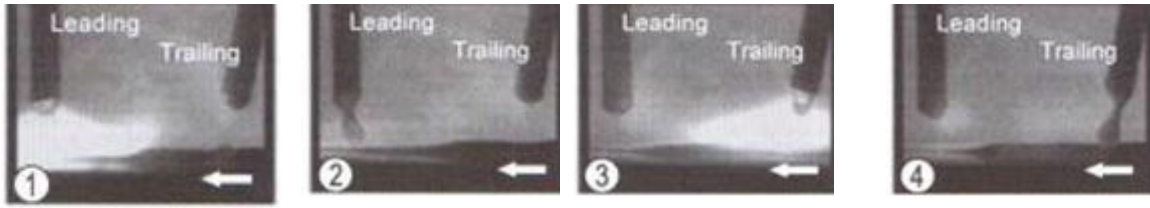


Figure 1.8: Functional principle of Time Twin Digital separate welding potential [28]

1.4.1 Metal transfer in Time twin weld-deposition

In the Time Twin weld-deposition processes the two electric arcs generated can be adjusted and optimized independent of one another. Both the performance and additional parameters - such as, the lengths of the two electric arcs can be controlled separately, which means that it is possible to achieve a stable electric arc and perfect drop release for both electric arcs. Two electrodes can be defined as the master and the slave. This means that the electrode which has the leading role in the welding process is not fixed. As a result of that, both welding directions are possible and this in turn enables a reduction in the cycle time. Figure 1.9 shows how metal is transferred and welding-current time curves in a twin wire welding process





- (1) Active arc – leading wire electrode (2) Metal transfer – leading wire electrode (3) Active arc – trailing wire electrode (4) Metal transfer – trailing wire electrode

Figure 1.9: Schematic representation of the metal transfer and welding-current time-curves for Twinwire

1.4.2 Welding speed and deposition rate

Using the Time Twin, it is possible to achieve considerable increases in the deposition rate compared with conventional electric arc welding processes. The user can convert this higher deposition rate either into a higher welding speed or into a greater cross-sectional area of the seam. In most applications, the increase in welding speed is of chief significance. The exact factor by which the welding speed can be increased depends on the material, the thickness of the sheet metal, the geometry of the seam, the welding positions etc.

1.5 Residual stresses

Residual stress is defined as “the stress resident inside a component or structure after all applied forces have been removed”. *Compressive* residual stress acts by pushing the material together, while *tensile* residual stress pulls the material apart. Mathematically, compressive stress is negative and tensile stress is positive. Stresses can also be characterized as normal stresses that act perpendicular to the face of a material and the shear stresses that act parallel to the face of a material. There are a total of 6 independent stresses at any point inside a material (3 normal and 3 shear stresses).

The total stress experienced by the material at a given location within a component is given by the sum of the residual stress plus the applied stress. Therefore, the knowledge of the residual stress state is important to determine the actual loads experienced by the component. In general, compressive residual stress in the surface of a component is beneficial. It tends to

increase the fatigue strength and fatigue life, decrease in crack propagation rate, and increase resistance to environmentally assisted cracking such as stress corrosion cracking and hydrogen induced cracking. Tensile residual stress in the surface of the component is generally undesirable as it decreases fatigue strength and fatigue life, increases crack propagation and lowers resistance to environmentally assisted cracking.

1.6 Problem Definition

The main constraint in producing the metallic components using additive manufacturing is residual stress that develops during the deposition process. These residual stresses decrease the strength and create deformation in products. Such products need to undergo the post process like heat treatment, shot peening etc. Before its actual use, these processes will change the property of the part produced and there by strength decreases further. Because of these reasons additive manufacturing is not being used for large scale production and fabrication of precise parts.

Residual stresses are the major issue in the AM process as it constraints the range of products that can be manufactured using the additive manufacturing process. The post production process like heat treatment and shot peening are undesirable due to the extra time involved. So the preferred option is by reducing the residual stress in the production stage itself. Since the technology is not matured enough modelling approach can be available option predict the outcome of the process. This will not only make the researcher and engineers understand the science behind the process but can easily make the process acceptable to industries.

As will be elaborated in the subsequent chapters, many numerical and statistical based modelling works has been reported regarding the formation of residual stresses in welding. But only few works has been reported in additive manufacturing using weld-deposition. Proper experimental and numerical study of residual stress in beam deposition with focus on the area-filling path can reduce these issues substantially.

In this thesis, an attempt is made to develop an algorithm to model weld-deposition AM infinite element analysis using ANSYS Mechanical ADPL. The same was used to analyse

the effect of area filling path patterns on the temperature gradient and the thermally induced residual stresses. The obtained results were then experimentally verified.

The main objective of present study is

- Residual stress distribution for zig-zag area-filling pattern to be modelled using FEA software (ANSYS Mechanical APDL).
- The modelling results to be verified experimentally using weld-deposition and the measurement of residual stress is being measured using X-Ray Diffraction.

1.7 Organization of Report

In *chapter 1* an introduction to the report is presented. It starts with emphasizing on what is Additive Manufacturing and weld based rapid prototyping. Problem statement with objective of present study is discussed later.

In *chapter 2* literature survey of various approaches to simulate welding and its application in additive manufacturing using finite element analysis are discussed.

In *chapter 3* an appropriate FEM approach to simulate the weld based additive manufacturing incorporating proper boundary conditions are explained and flow diagram of the analysis in ANSYS APDL is discussed.

In *chapter 4* experimental setup and procedures are discussed, later experimental and simulation results are validated.

In *chapter 5* conclusions and future scope is discussed.

Chapter 2

Literature Survey

2.1 Study on numerical modeling of welding

The basic theory of heat flow that was developed by Fourier and applied to moving heat sources by Rosenthal and Rykalin in the late 1930s is still the most popular analytical method for calculating the thermal history of welds [6]. During the 1940s and 1950s, the theory was extended and refined. One of the first presentations of the general theory of thermal stresses including non-linear phenomena is given in the comprehensive work by Boley and Weiner, 1960 [5]. Before the mid 1980's, limited computing power forced the numerical analysis to two-dimensional models though most welding situations result in fully three dimensional states of stresses and deformations. Later to overcome most of the limitations, several authors have used the finite element method (FEM) to analyze heat flow in welds.

The first three-dimensional transient heat transfer analyses were published in the mid 1980's. A few years later, the coupling to thermal stress analyses on quite simple models were feasible from a computer hardware point of view. The detailed three dimensional geometrical modelling of these local welding aspects was possible from a computational point of view compared to thermal stress analysis of the complete structure being welded [6]. In the mid 1990's, an increasing number of works have been published considering calculations of welding induced transient and residual stresses. In this context it should be noted that considerable commercial efforts have been put into making software packages such as ANSYS, ABAQUS, SYSWELD and etc for numerical simulation of welding applications.

2.2 Computational Welding Mechanics

The pioneering work within simulation of welding in the early 1970s, e.g. Ueda and Yamakawa [7] and Hibbit and Marcal[8], included material non-linearity and the coupling

between thermal and mechanical analysis. Experts have demonstrated that MARC, developed by Marcal and Hibbit, and ABAQUS, developed by Hibbit, are among the most highly regarded commercial FEA-software for nonlinear problems. One of the most comprehensive reviews in Computational Welding Mechanics (CWM) is done by Lindgren [9]. The scope of Computational Welding Mechanics is to establish methods and models that are usable for control and welding of welding processes to obtain optimal mechanical performance [10]. The phenomena that are relevant in the welding can be divided in different fields, shown in Figure 2.1. It has been found that it is possible to decouple the modelling from the physics of the welding process by ignoring fluid flow in CWM and still being able to create models fit for purpose.

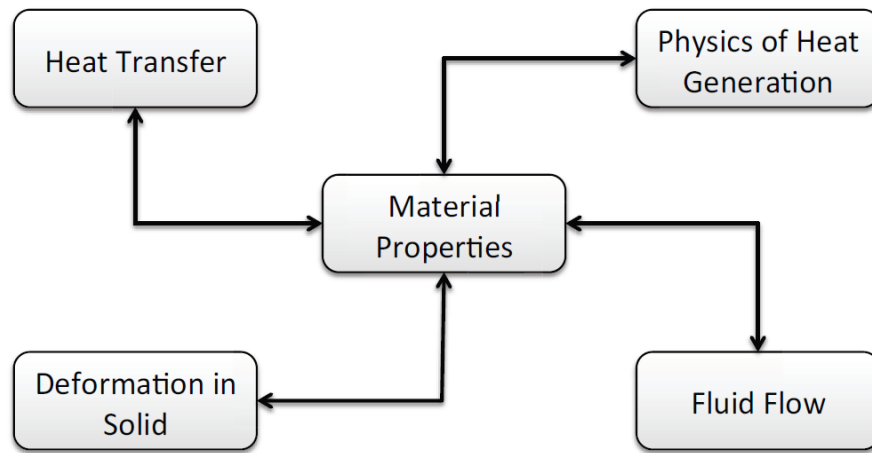


Figure 2.1: Different domains of CWM [6]

2.3 Study on residual stresses developed during weld-deposition

A three-dimensional (3D) finite element model was developed to investigate thermally induced stress field during hybrid laser–gas tungsten arc welding (GTAW) process [11]. A series of experiments were performed to validate the numerical results and found that compared to the welded joint obtained by GTAW and laser welding alone, the residual stress concentration in the weld joint obtained by hybrid laser–GTAW is the minimal one. The temperature history and the residual stress in multi-pass butt-welded stainless steel pipe was analyzed by Feli et.al [12]. The 3D finite element model was developed using ABQUS [13] and experimental validation was done using Hybrid laser-GMAW system and the residual stress has been measured using x ray diffraction technique. The different components of

residual stress obtained with respect to welding speed were compared with the experimental results. Using double-ellipsoid heat source the transient temperature distributions of the welded plates were generated by Grey [14].

A finite element analysis model using element activation has been developed to simulate the mechanical and thermal phenomena in FDM and further used for residual stress and part distortion simulations [15]. The model has also been used to study the tool-path effects on the FDM process. The tool-path patterns affect the residual stresses in not only the magnitude but also the distribution which shows stress concentrations aligned with the primary direction of the tool path. From the simulations, it is also shown that the short-raster tool path results in higher residual stresses, and thus possibly larger distortions, than the long-raster and alternate-raster patterns, both having similar stress distributions and distortion features. A number of assumptions have been followed for creating the finite element model by Babu and Kishore [16], for numerical simulation of welding. In order to obtain these results they have investigated the effect of arc welding on bead geometry using the finite element simulation of hybrid welding process on 304 austenitic stainless steel. A new finite element model for welding heat sources is attempted by J. Goldak et.al [17]. In this paper a mathematical model for weld heat sources based on a Gaussian distribution of power density in space is presented. In particular a double ellipsoidal geometry is proposed so that the size and shape of the heat source can be easily changed to model both the shallow penetration arc welding processes.

Investigation of residual stresses in the laser melting of metal powders in the additive layer manufacturing is done by Ibiye Asebichin Roberts [18] in this thesis work. In his work, the effects of process and material variables on the residual stress distributions in the laser melting of Ti64 powder were discussed and reported. The ultimate goal was to augment with practical experience and minimise the need for cost intensive experimental fabrication for the purpose of understanding the effects of process parameters. Laser direct metal deposition (LDMD) of dissimilar and functionally graded alloys was attempted by kamran shah [19]. The aim of this work was to understand and explain mechanisms occurring in diode laser deposition of dissimilar materials and functionally graded materials. First part of this work addressed diode laser deposition of Inconel 718 nickel alloy to Ti-6Al-4V titanium alloy and in second part of this study; an image analysis technique had been developed to measure the

surface disturbance and the melt pool cross section size during laser direct metal deposition of Inconel 718 on a Ti-6Al-4V thin wall

Sudersanan & Kempaiah[20] have studied the residual stress induced in the dual phase steel with changes in heat input and travel speed during butt welding. Multi pass butt welding was carried out on DP Steel specimens using MIG welding. The residual stress in the weld metal, heat affected zone and base metal were measured using X-ray diffraction technique. A sequentially coupled thermo mechanical analysis was carried out using ANSYS to validate the result. The analysis showed good agreement with the experimental result. Further analysis using the validated FEM model was carried out to investigate the effect of heat input on welding residual stress. The result showed a significant increase in residual stress with the increase in heat input and decrease with the increase in travel speed. Finite element method is used to develop an efficient and reliable method for simulation of the welding process by Rajlaxmi & Jadhav [21]. The molten state of the weld pool is presented by the moving heat source. The element birth and death technique was introduced to represent the melting of the material. A numerical simulation of the welding induced temperature field and corresponding distortions helps to investigate the heat effects of welding and, in the long run, to optimize the quality of welded parts. Due to the complexity of the welding process itself, the material property data for the simulation has to be temperature and phase dependent. The analysis results help us understand the phenomena governing the welding of a joint, offering insight on the mechanisms and mechanical aspect particular to the welding process. Whereas Ameen et.al. [22] studied the relation between heat flux input and residual stress. They examined the influence of residual stress on butt weld; an experiment was performed using the TIG welding setup, for different 'v' angles such as 30°, 45°, 60°, 90°. In his work the numerical result obtained from finite element software ANSYS Mechanical APDL is validated using experiment, and concludes with the relation between the heat flux input and residual stress.

A three-dimensional model was used to simulate laser welding of two stainless steel plates [23]. The heat input was simulated as a moving heat source. Elements were activated along the welding path in order to account for the joining of the material. Large deformations, temperature dependent material properties, volume changes due to phase changes are included in the model. Experiments have been performed in order to evaluate the accuracy of

the model. A 3-D finite element model for the prediction of the distortion and residual stresses induced during electron beam welding is described in [24]. The model is validated by butt welding experiments on two Inconel 718 plates. A particular effort is made to determine a good model for the heat input. A combined conical and double ellipsoid heat source is used to model the deep penetration characteristic of the electron beam and this source is calibrated using the results from a separate thermodynamic simulation, using the finite difference code. Parallel computation is used to reduce the overall simulation time in the coupled thermo mechanical simulation of welding. The agreement between calculations and experiments is good with respect to the residual stresses. Measured and computed deformations agree qualitatively although they differ in magnitude.

2.4 Studies on temperature field and stress distributions during weld based additive manufacturing

A three-dimensional finite element model with temperature-dependent material properties was investigated to find temperature field and thermal stress distributions in multi-pass single-layer weld-based rapid prototyping. The experiments of multi pass single-layer weld-based rapid prototyping were carried out to measure the thermal cycles and residual stress distributions of the depositing component by H. H. Zhao et.al. [25]. The results show that in the depositing process of multi-pass single-layer weld-based rapid prototyping, the rear pass has the stress release effect on the fore passes, and the non-uniform multi-peak thermal cycle experienced during the depositing is the main cause of the stress release effect. The stress of the last pass plays a significant effect on the residual stress distribution of the whole component. M. P. Mughal et.al. [26] performed a 2D finite element thermo-mechanical model to predict the residual stress induced deformations with application to processes where material is added using a distributed, moving heat source. A sequentially coupled thermo-mechanical analysis was performed using a kinematic thermal model and plane strain structural model. The simulation results were compared with experimental data for successive sections along deposition and it was found that, with the exception of deposition center and plate edges, the two are in very good agreement.

2.5 Study on temperature field during Twin Wire welding

Q.G. Meng et.al [27] analysed the shape of twin wire welding's arcs and the track of droplets transition and found that the twin wire welding's fore arc and rear arc all deflect to the middle of the two arcs. Based on this the double ellipsoid heat source model is modified, and a heat source model which can apply to calculate the twin wire welding's temperature field is put forward. This model is testified by actual experiment of temperature sampling. By comparing the temperature field of twin wire welding and single wire welding, the results show that twin wire welding has slender weld pool the end part of which is ellipsoid, and its HAZ is narrower than that of single wire welding.

Summary

In this chapter the history of finite element modelling of welding are referred. The finite element analysis can be done using number of general FEA software's such as ANSYS, ABAQUS and dedicated weld modelling software's like SYSWELD, MORFEO and SIMUFACT WELDING etc. Using these packages various factors that affect the residual stress are studied and are generalized. Along with the welding process, numbers of studies are done on various issues in weld based rapid prototyping techniques in which, residual stress was found to be the major factor and various studies are done on warping mechanism due to residual stress in additive manufacturing of metallic objects.

Chapter 3

Finite Element Modeling of Weld-deposition

3.1 Introduction

Finite Element Method (FEM) is widely used numerical technique for finding approximate solutions to boundary value problems for equations. In this chapter the finite element modeling of the welding process is divided into four parts. In the first part a brief introduction to the finite element method and its general procedure for solving weld problem is presented along with the governing equations and the boundary conditions. The second part includes the material model used and modeling of the heat source of twin wire welding. The third and fourth parts include filler material addition and deposition modeling procedures.

3.2 Thermo-Mechanical Analysis of Welding

In welding application, the magnitude of the heat generated by the plastic deformation is less than that of heat generated by the heat source during welding. Therefore, a sequential thermal and mechanical numerical analysis can be applied. The most frequently adopted approach of two step thermo-mechanical calculation is applied in the present work. Following is the basis of the sequential thermo-mechanical analysis. At first, the thermal analysis is carried out to calculate the time-temperature distribution in a non-linear heat transfer analysis. The heat input into the work piece is approximated by a moving heat source and filler material addition performed at an initial temperature well above the liquidus temperature. Subsequent to the thermal analysis, the temperature field is used as a thermal load in a non-linear mechanical analysis to calculate the mechanical effects on the work piece due to thermal strains.

3.3 Governing Equations and Finite Element Evaluation

3.3.1 Thermal Analysis

Fourier law states the governing equation for heat conduction, the (transient) governing equation for temperature becomes

$$\rho c_p \frac{\partial T}{\partial t} = \frac{\partial}{\partial x} \left(\frac{\partial T}{\partial x} \right) + \frac{\partial}{\partial y} \left(\frac{\partial T}{\partial y} \right) + \frac{\partial}{\partial z} \left(\frac{\partial T}{\partial z} \right) + Q_v \quad (3.1)$$

Where T Temperature

ρ Material Density

C_p Specific heat

K Heat Conductivity

Q_v External Volumetric Heat supplied into the body

3.3.2 Mechanical Analysis

The mechanical model based on the solution of the three governing partial differential equations of force equilibrium. In tensor notation, these are written as

$$\sigma_{ij,i} + p_j = 0 \quad (3.2)$$

Where p_j Body force at any point

σ_{ij} Stress tensor

3.4 Boundary Conditions

3.4.1 Thermal Boundary Conditions

Applying proper boundary conditions for weld-deposition is very much essential. There are mainly three boundary conditions considered for thermal problems i.e. ambient temperature, convection and radiation. The boundary condition for thermal analysis for weld-deposition at a single point is shown in fig 3.1.

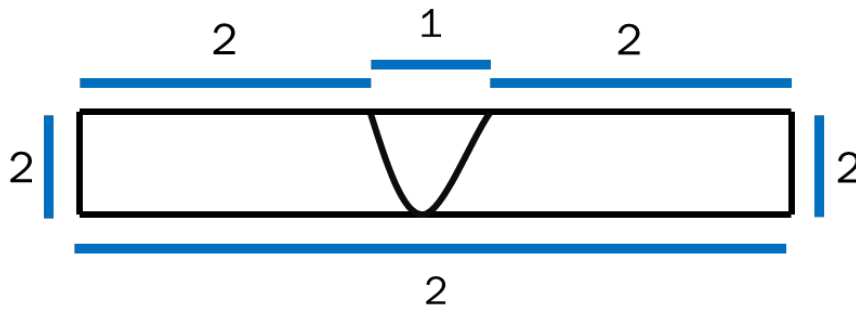


Figure 3.1: Boundary condition for thermal analysis

1. Heat Input

2. Convection and radiation

- According to Newton's Law surface convection heat loss is given by

$$q_{con} = h_{con} \cdot (T - T_0) \quad (3.3)$$

Where h_{con} Convection heat transfer coefficient

T_0 Ambient temperature

- According to Stefan-Boltzmann's law the radiation heat loss is given by

$$q_{rad} = \varepsilon \cdot \sigma \cdot ((T - T_Z)^4) - ((T_0 - T_Z)^4) \quad (3.4)$$

Where ε Emissivity constant

σ Stefan-Boltzmann constant

T_Z Absolute zero on the actual temperature scale

3.4.2 Mechanical Boundary Conditions

If one material is heated uniformly having all degrees of freedom unconstrained, then the body regains its original shape if it is cooled uniformly, but this does not occur in deposition process as the cooling is not uniform. The area adjacent to the recently deposited weld bead will be having higher temperature than that of other. Thereby expansion and contraction will be non-uniform, resulting in inducing stress within the body. But if the base plate is having

all degrees of freedom are not restricted, then the stress will be relieved on cooling down by deforming the base plate. But this phenomenon is not desirable so the degree of freedom all four boundaries of the plates should be constrained in all the direction as shown in fig 3.2 so that the residual stress retains inside the plate while cooling down.

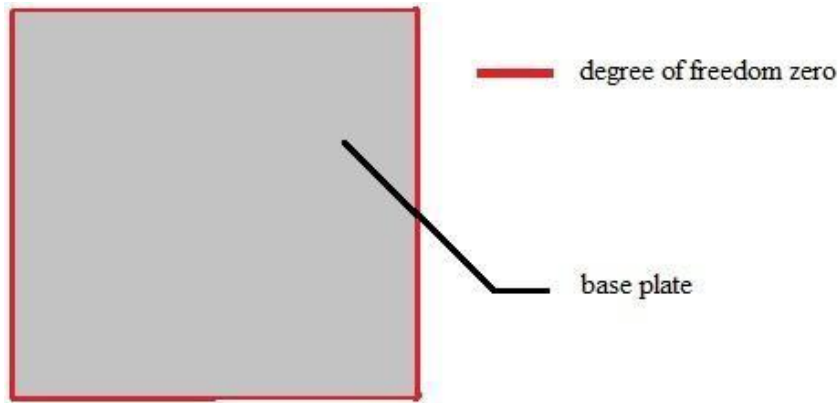


Figure 3.2: Boundary conditions for structural analysis

3.5 Modeling of Heat Source

Due to highly non-uniform temperature field applied during welding the residual stresses and deformation in welded structures are formed. It is well-known fact that both the residual stresses and welding deformations are highly sensitive to transient temperature distribution. Thus determination of realistic temperature profile in the target application is required for a very careful and accurate modelling of heat source. In welding an electric arc, approximately 60-70% of the heat energy is generated at the anode and the rest at the cathode.

The net heat input (per unit of time) and is given by

$$Q = \eta UI \quad (3.5)$$

Where	Q	Heat Input (W)
	η	Arc Efficiency (%)
	U	Voltage (V)
	I	Current (A)

The most widely acceptable model for simulation of arc welding process is the doubled ellipsoidal heat source model, presented by Goldak et.al. [13], is used in the present work. This model gives Gaussian distribution and has excellent feature of power density distribution control in the weld pool and HAZ. The heat input is defined separately over two regions; one region in front of the arc center and the other behind the arc center, shown in figure 3.3.

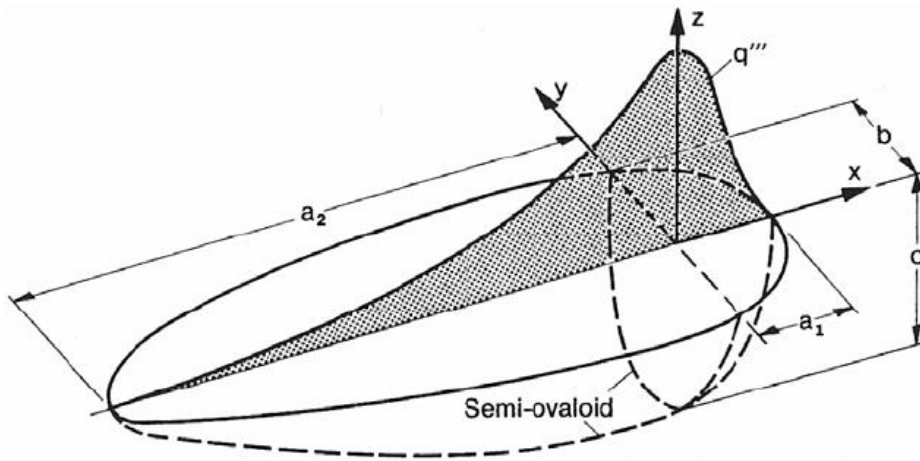


Figure 3.3 : Double ellipsoidal heat source model [17]

The heat distribution of front and rear quadrants of the heat source of welding arc is expressed as [3.5 & 3.6][16]

$$q_f = \frac{6\sqrt{3}\eta Q f_f}{\pi\sqrt{\pi}a_f bc} e^{-3\left\{\left(\frac{x^2}{a_f^2}\right)+\left(\frac{y^2}{b^2}\right)+\left(\frac{z^2}{c}\right)\right\}} \quad (3.6)$$

$$q_r = \frac{6\sqrt{3}\eta Q f_r}{\pi\sqrt{\pi}a_r bc} e^{-3\left\{\left(\frac{x^2}{a_r^2}\right)+\left(\frac{y^2}{b^2}\right)+\left(\frac{z^2}{c}\right)\right\}} \quad (3.7)$$

Where $Q = VI$ $f_f + f_r = 2$

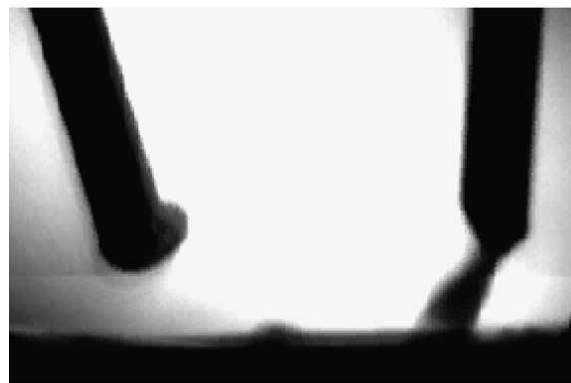
a_r, a_f, b, c are characteristic parameters of heat sources.

3.5.1 Heat source modelling of twin wire welding

By analyzing the shape of twin wire welding's arcs and the track of droplets transition, the phenomenon that the twin wire welding's fore arc and rear arc all deflect to the middle of the two arcs is found. Based on this the double ellipsoid heat source model is amended, and a heat source model which can apply to calculate the twin wire welding's temperature field is put forward by Q.G.Meng et.al.[27]. In the existing models, double ellipsoid heat source model is more suitable to MIG welding[15]. But twin wire welding's temperature field calculated by this model has more errors with experimental results [16]. In order to know the reason for errors, twin wire welding's arc shape is analyzed experimentally and the track of droplets transiting is observed. Fig. 3.4 shows the fore wire and rear wire droplets transiting process when welded with twin wire welding. It is obvious that both arcs droplets deflect to the middle at the time of transiting.



(a)



(b)

Figure3.4: Droplets transiting track of twin wire welding [27]. Droplets transiting of (a) Fore wire and (b) Rear wire

3.5.2 Modification of heat source formula

Q.G.Meng et.al. [27] has found that arc's deviation in other words refers to weldment deviating at a certain degree. To double ellipsoid heat source model, according to the arc deflecting rules gained from the analysis of arcs shape the weldment should deflect around the width direction of weld pool. In Fig. 3.5, weldment deflection of an angle β around Y axle in anti clock wise direction is shown. Where X is the welding direction, y is the width direction of weld pool, and z is the penetrating direction.

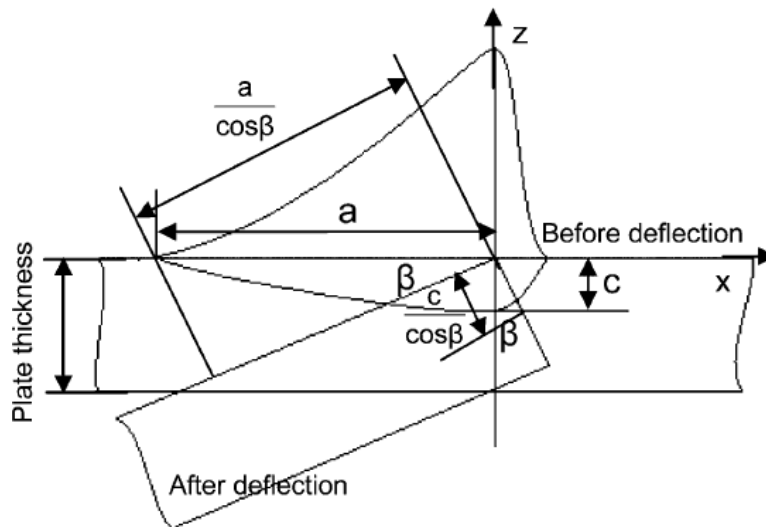


Figure3.5: The revolute diagrammatic sketch of double ellipsoid heat source model [27]

The modified equation of heat source is:

The former half part of the ellipsoid:

$$q_f = \frac{6\sqrt{3}\eta Q f_f \cos^2 \beta}{\pi \sqrt{\pi} a_f b c} e^{-3 \left\{ \left(\frac{x^2}{\left(\frac{a_f}{\cos \beta} \right)^2} \right) + \left(\frac{y^2}{b^2} \right) + \left(\frac{z^2}{\left(\frac{c}{\cos \beta} \right)^2} \right) \right\}} \quad (3.8)$$

The rear half part of the ellipsoid

$$q_r = \frac{6\sqrt{3}\eta Q f_r \cos^2 \beta}{\pi \sqrt{\pi} a_r b c} e^{-3 \left\{ \left(\frac{x^2}{\left(\frac{a_r}{\cos \beta} \right)^2} \right) + \left(\frac{y^2}{b^2} \right) + \left(\frac{z^2}{\left(\frac{c}{\cos \beta} \right)^2} \right) \right\}} \quad (3.9)$$

Where

$$Q = VI$$

$$f_f + f_r = 2$$

a_r, a_f, b, c are characteristic parameters of heat sources and β is the deflecting angle.

Characteristic parameters of heat sources are taken as follows:

$$\begin{array}{l|l|l|l} f_f = 0.6 & f_r = 1.4 & \eta = 0.7 & \\ a_f = 3 \text{ mm} & a_r = 9 \text{ mm} & b = 5 \text{ mm} & c = 4 \text{ mm} \end{array}$$

Deflecting angle (β) for fore wire's arc is taken as 40° and 30° for back wire's arc.

3.6 Filler metal deposition

The welding process can be performed with or without filler material depending on which process used and the requirement on the weld geometry. Modelling of filler material is very important issue in computational weld mechanics because of its effects on the final thermo-mechanical effects on the geometry and properties. In numerical simulation of welding, deposition of filler material is modelled by using three different approaches[17],

1. Element movement technique
2. Inactive element technique
3. Quite element technique

In quiet elements the elements are present during the whole analysis but the stiffness and the thermal conductivity is very low so that they do not disturb the rest of the model. They are activated simply by giving them correct material properties. With the other method, inactive element, the elements are not part of the system of equations until they are activated. In our present work we will use quite element technique for which ANSYS has special feature called element birth and death functionality. In the quite element technique the elements belonging to filler metal are deactivated by assigning them a very low thermal conductivity (in thermal analysis) and very low stiffness (in structural analysis). The value of thermal conductivity and stiffness of deactivated elements should be low as these may not have any contribution in the rest of the model but should not be as low which may produce an ill conditioned matrix. The elements belonging to a specific weld bead are reactivated by "element birth" option at the

start of the respective weld bead or when they come under the influence of welding torch. The material properties of reactivated elements are instated at the time of their activation.

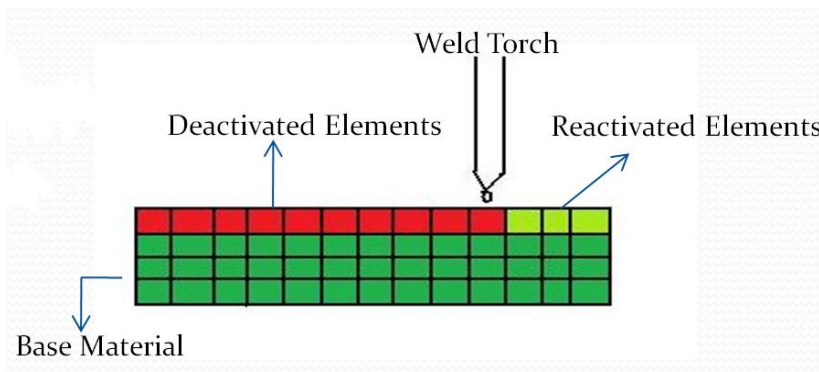


Figure 3.6: Filler metal deposition in simulation of welding operation

3.7 Material Properties

The temperature-dependent material properties of the substrate are also used for depositing metal. The filler metal was mild steel with AWS designation as ER70S-6 wire while the base plate is mild steel. Complete ranges of material properties for this adopted at different temperatures are taken from Karlsson and Josefson [29] shown in Fig. 3.7[a &b].

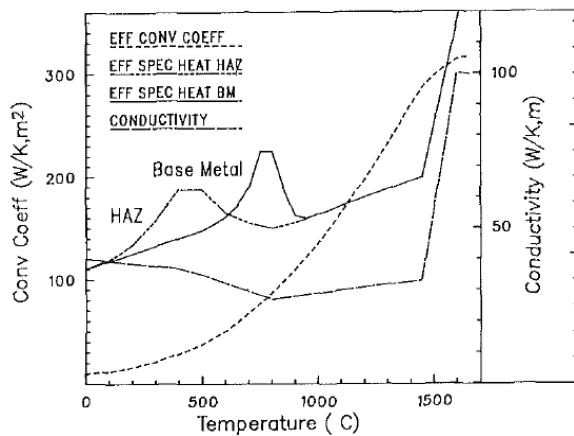


Figure3.7 (a):Thermal material properties for steel considered

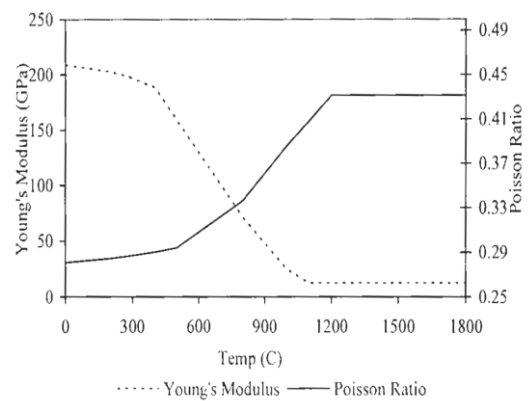


Figure 3.7 (b):Young's modulus and Poisson Ratio as function of temperature

3.8 Application of Heat generation

Double ellipsoid heat equation discussed above is used to generate heat at the centroid of the each element which is activated. The time for heat generation at each element is calculated as follows

$$t = \frac{\text{Length of deposition}}{\text{Welding Speed}} = \frac{LD}{S} \quad (3.10)$$

Before entering into the solution phase during simulation of multi pass single layer weld based additive manufacturing, we deactivate the deposition elements and later each element will be activated according to deposition pattern i.e. zig-zag raster path and heat generation is applied at the center of the each activated element as the heat source moves forward.

The chemical composition of the welding wire used is as follows

Table 1 : Chemical composition of ER70S-6 wire

Carbon:	0.06 – 0.15%	Chromium:	0.15 %
Manganese:	1.40-1.85 %	Copper:	0.50 %
Sulfur:	0.035 %	Silicon:	0.80 – 1.15 %
Nickel:	0.15 %	Phosphorus:	0.025 %
Vanadium:	0.03 %	Molybdenum:	0.15 %
Iron:	Balance	Other Totals:	0.50

3.9 ANSYS Analysis Procedure

The ANSYS parametric design language (APDL) is used to develop a subroutine for solving twin wire welding problem for zig-zag path, here coupled thermo-mechanical analysis is performed. The sequential thermo-mechanical simulation strategy is as follows see figure 3.8.

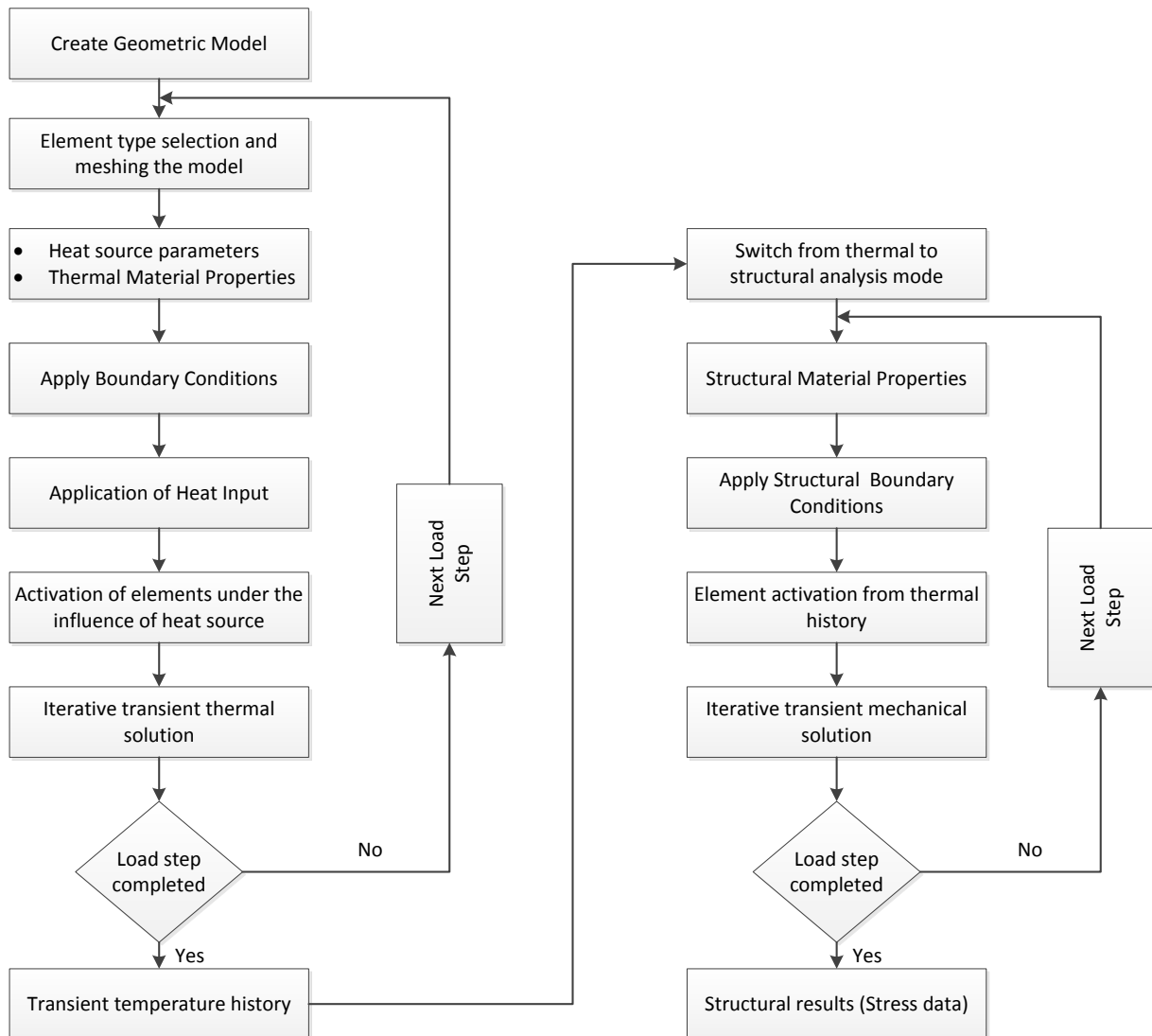


Figure 3.8: Detailed sequentially coupled thermo-mechanical ANSYS analysis

A 3-D finite element model of a single-layer rapid prototyping process is presented to study the temperature field and thermal stress distributions using twin wire welding. The geometric model and finite element mesh is shown in Fig. 3.9. X direction stands for the width direction, Y direction is the thickness direction, and Z direction is the depositing direction. The FE model consists of 25000, 3D Solid-70 elements. The deposition area is fine meshed. The double ellipsoid heat source model with a modification is used as the depositing heat source model [27]. The elements of the depositing passes are deactivated initially before the solution phase and activated gradually during the depositing process. The initial temperatures of all nodes are set to be the ambient temperature 298K. The mechanical boundary condition is loaded in the principle of no rigid component movement along the border of work piece.

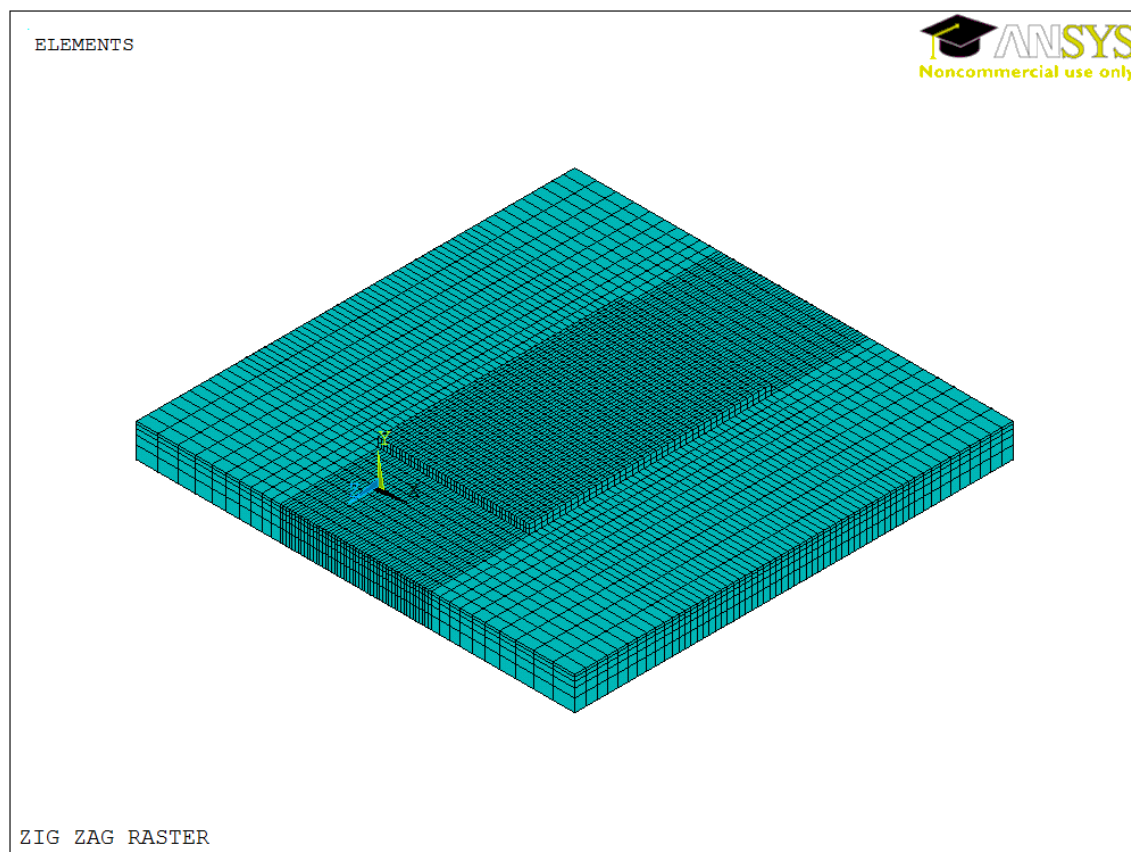


Figure3.9: Three-dimensional finite element model

3.9.1 Assumptions during Thermal and structural modeling in ANSYS

- Overlap of heat source of each pass is 50%.
- Convection due to shielding gas is not modeled.

- A thermal insulation is kept between the fixture and base plate to avoid conduction through clamps.
- Strain hardening and creep are not included in material model.
- Degree of freedom of four boundaries of base plate is constrained.
- Initially work piece (base plate) is at ambient temperature.

3.10 Simulation Results

The temperature field distribution of the base plate when the heat source is at middle of 1st, 4th, 9th passes are presented in Figure 3.10 (a, b & c). Heat is gradually accumulated and the temperature region becomes larger. First pass will pre-heat the base plate for second pass and so on.

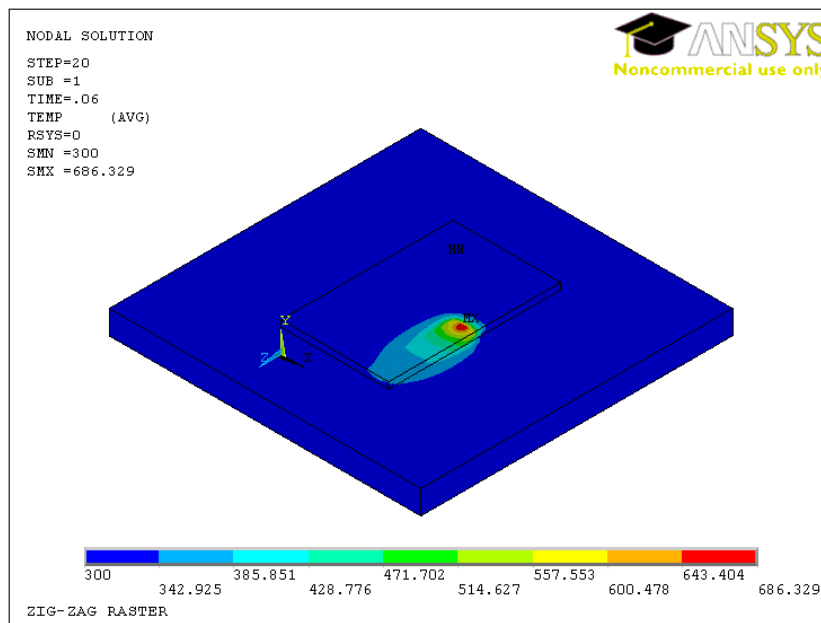


Figure 3.10 (a): Temperature distribution of 1st pass when source is at middle

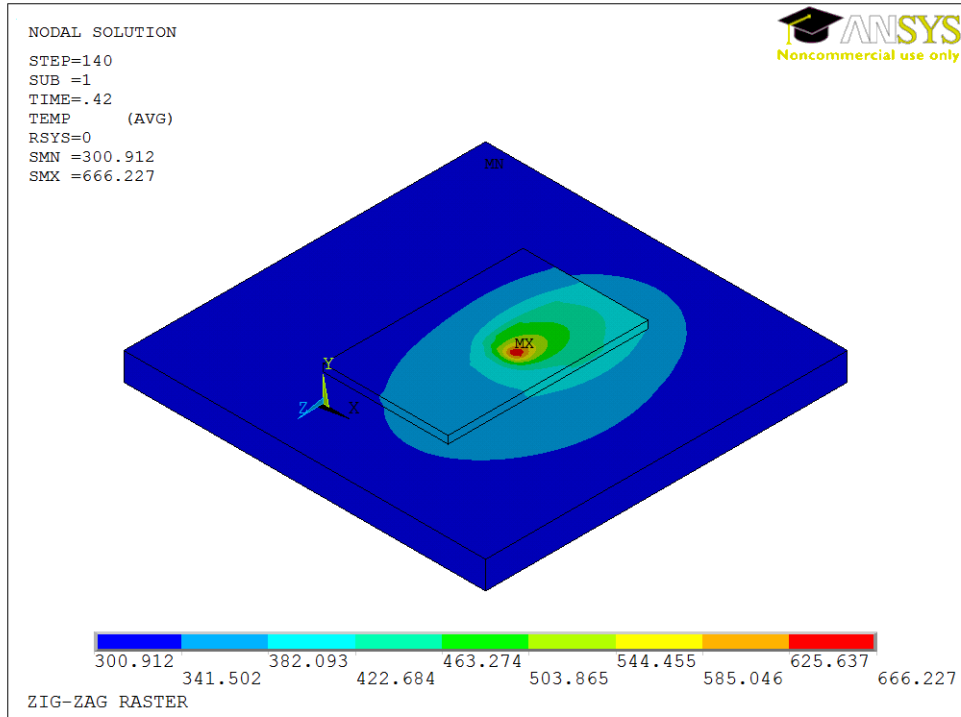


Figure 3.10 (b): Temperature distribution of 4th pass when source is at middle

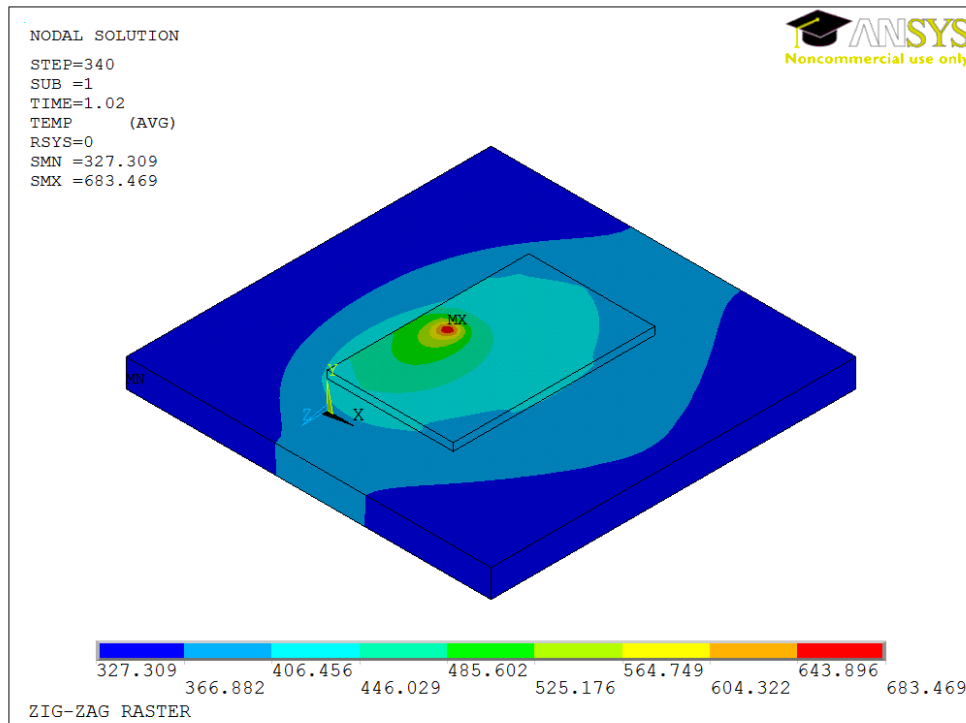


Figure 3.10 (c): Temperature distribution of 9th pass when source is at middle

Chapter 4

Experimental Validation

4.1 Introduction

An experimentation is carried out to validate the finite element model. The deposition system and the general methodologies of the experiments required for the model verification are discussed in this chapter. The fixture prepared to carry out residual stresses measurement and detailed procedures required for residual stresses measurement is also discussed.

4.2 Experimental setup and procedure

The entire experiment is performed using Time twin welding (MIG). The experimental validation procedure is explained under the following headings:

1. Setup of depositing system
2. Design of fixture
3. Experimental procedure
4. Measurement of residual stresses

4.2.1 Setup of depositing system

Two TransPuls Synergic (TPS) weld-deposition unit integrated with the Robot machine is used to out carry tests for validating finite element model. Single layer of deposition is used for the thermal and structural verification of the present finite element model while multi layered deposition is left for future scope. Figure 4.1 and 4.2 shows the weld-deposition setup.

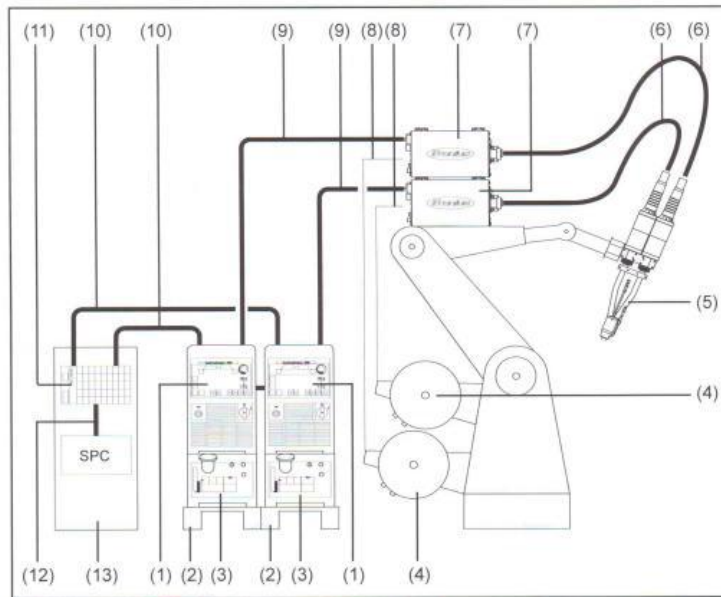


Figure 4.1: Simple drawing of welding set up and wire spool connecting with robot [28].

- | | |
|--------------------------------|--|
| (1) TPS 5000 power source | (8) Wire feed hose |
| (2) Base stand | (9) Standard interconnecting cable |
| (3) Cooling unit | (10) Remote-control cable |
| (4) Wire spool holder on robot | (11) Twin Standard I/O job robot interface |
| (5) Twin 500 welding torch | (12) Cable connector to robot control |
| (6) Twin torch hose pack | (13) Robot control |
| (7) Robot wire feeder | |



Figure 4.2: Welding deposition system integrated with Robot machine

4.2.2 Power source

Power sources for the Time Twin compared with the power sources previously were converted to all-digital technology. The innovative feature of this is that, now, it is possible to control the welding process in a completely digital manner. A digital signal processor (DSP) takes care of this control. The analogue welding voltage / analogue welding current are registered on the electric arc. These analogue values are converted to digital signals by an analogue-to-digital converter which feeds the digital signals to the DSP. The DSP then controls the welding process so as to adjust the actual values to the desired / nominal values.

Figure 4.3 shows the power source of time twin welding.



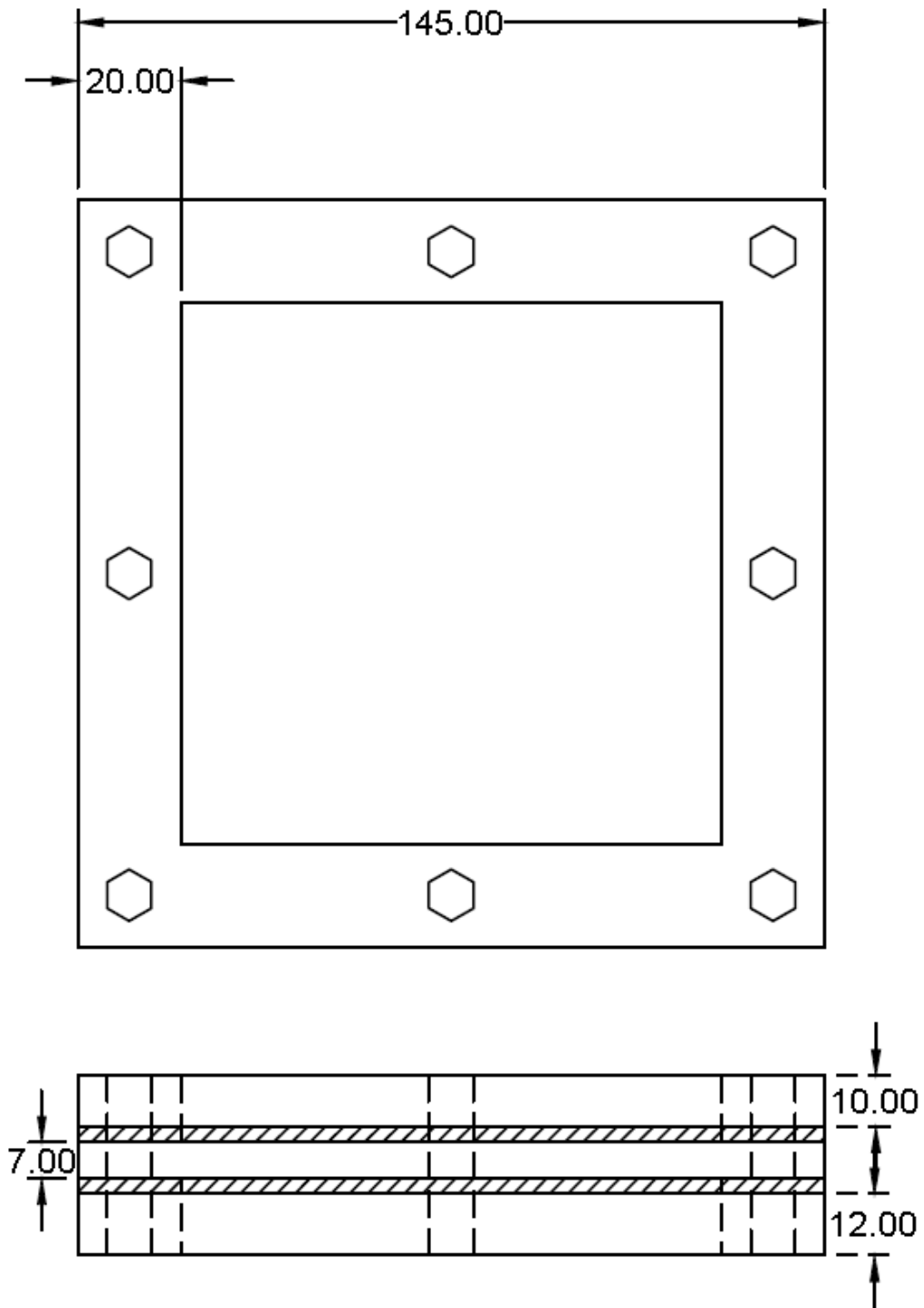
Figure 4.3: Complete welding system based on the power source Time Twin Digital 5000

4.2.3 Design of fixture

During experiment, if the specimen is allowed to cool down with full degree of freedom then the residual stress induced within the material will try to relieve due to warping of the base plate, this condition is not desirable hence fixture is to be designed in order to retain the stress. The considerations that are to be done for fixture design are:

- 1) Equal and uniform force should be exerted throughout the boundary of the plate.
- 2) Proper clearance should be provided for the movement of the weld torch and for the movement of the XRD probe for residual stress measurement.
- 3) Deposited area of the base plate and its bottom surface should not be in any contact with any other material (i.e. Heat loss is through convection only)
- 4) The fixture should withstand the force exerted due to the induced residual stress.

Fixture consists of two hollowed square plates which sandwiches the workpiece and square cut welding apron is used as the thermal insulator to avoid the heat conduction through clamps. The fixture is tightened using eight align screws. The fixture design in AUTOCAD is shown in fig 4.4 and fig 4.5 shows different views of the fixture.



Note: All dimensions are in mm

Figure 4.4: AUTOCAD figure of Fixture



Figure 4.5: Different orientation of fixtures before and after the deposition

4.2.4 Experimental procedure

Experiment was performed to compare the numerical results with experimental results obtained by manufacturing a single layered specimen with conditions and parameters similar to what was used for finite element analysis. The residual stresses estimation was also compared against the experimentally determined residual stresses obtained using XRD technique and that will be discussed further in this chapter.

The process parameters used for depositing single layer weld-deposition on base plate in zig-zag raster area filling path, see table 2. The base plate is OD dimension $145 \times 145 \text{ mm}^2$ in which after its being assembled in fixture the total surface area left will be $105 \times 105 \text{ mm}^2$ in that after giving enough space for torch movement area filling weld-deposition is done on $60 \times 30 \text{ mm}^2$. Weld-deposition in the above mentioned area filling path is shown in fig 4.6. The results obtained are discussed in the following section.

Table 2: Process Parameters

Parameters	Description
Current	112A
Inert gas	82% of Argon + 18% of CO ₂
Gap between two wires	5 mm
Gap between base to nozzle	18 mm
Filler material used	Copper coated mild steel wire (ER70S-6)
Filler wire diameter	12 mm each
Weld torch speed	0.6 m/min
Percentage of overlap	50%
Gas flow rate	12 lit/min

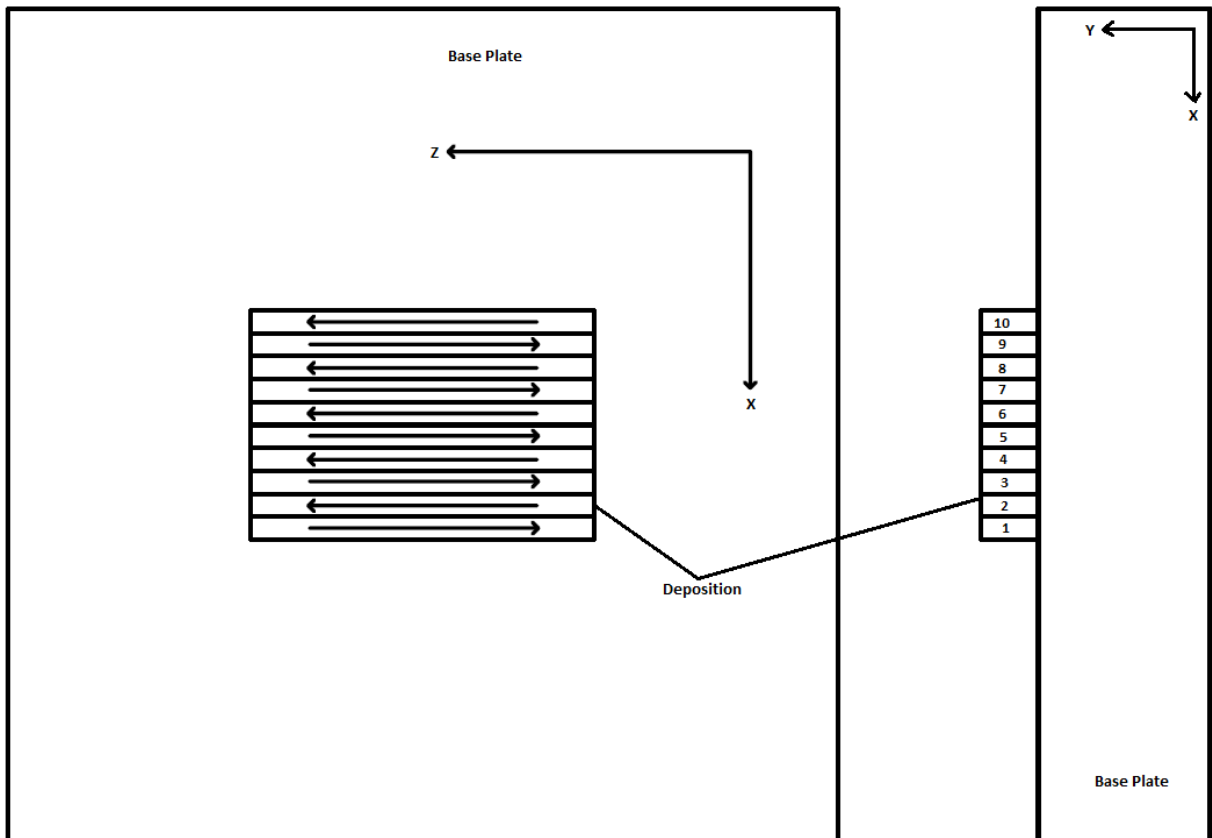


Figure 4.6 : Experimental Setup of base plate and Deposition Sequence

4.2.5 Measurement of residual stresses

Residual stresses were measured using proto XRD residuals stress measuring instrument shown in fig 4.5 on the back side of the specimen that was used to deposit the multi-pass single-layer weld before and after the deposition process for which uses x-ray diffraction technique to measure the residual stress. The residual stresses predicted by the finite element model were then compared with experimentally determined residual stresses.

In x-ray diffraction residual stress measurement, the strain in the crystal lattice is measured, and the residual stress producing the strain is calculated, assuming a linear elastic distortion of the crystal lattice. Diffraction occurs at an angle 2θ , defined by Bragg's Law: $n\lambda = 2d \sin \theta$, where n is an integer denoting the order of diffraction, λ is the x-ray wavelength, d is the lattice spacing of crystal planes, and θ is the diffraction angle. In our experiment the range of beta angle assigned for this measurement is from -20° to 20° and the properties assigned are of ferrous materials. Total number of points selected for measuring residual stress is 10 over a length of 80mm.

The accuracy of the method depends upon the efficiency with which the above mentioned procedures are carried out like proper surface preparation, correct selection of installation of specimen and proper selection of beta angles.

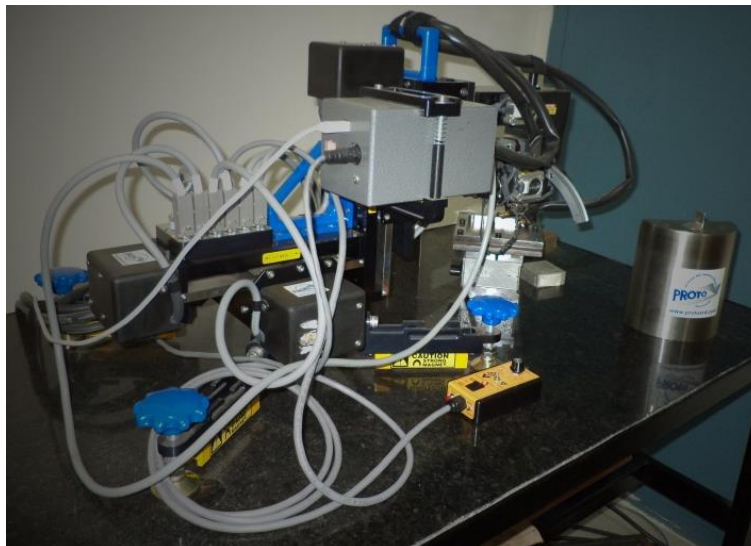


Figure 4.7: X-Ray Diffraction residual stress measurement instrument

4.3 Comparison of experimental and simulation results

Three-dimensional finite element model result is compared against experimental data. Diameter of each mild steel welding wire is 1.2 mm (twin wire) of AWS designation ER70S-6, are used to build a layer of deposition of 60 x 30 x 2.0 mm on the base plate using CO₂ and argon as the shielding gases. A zig-zag raster deposition pattern is used along Z-direction. The deposition starts at the lower left corner of the area indicated as deposition area in Figure 4.4 and ends at the upper left corner.

The experimentally determined residual stresses are compared with the numerical prediction along diagonal (Line 1) and axially (Line 2) on back side of the base plate, as shown in Figures 4.8.

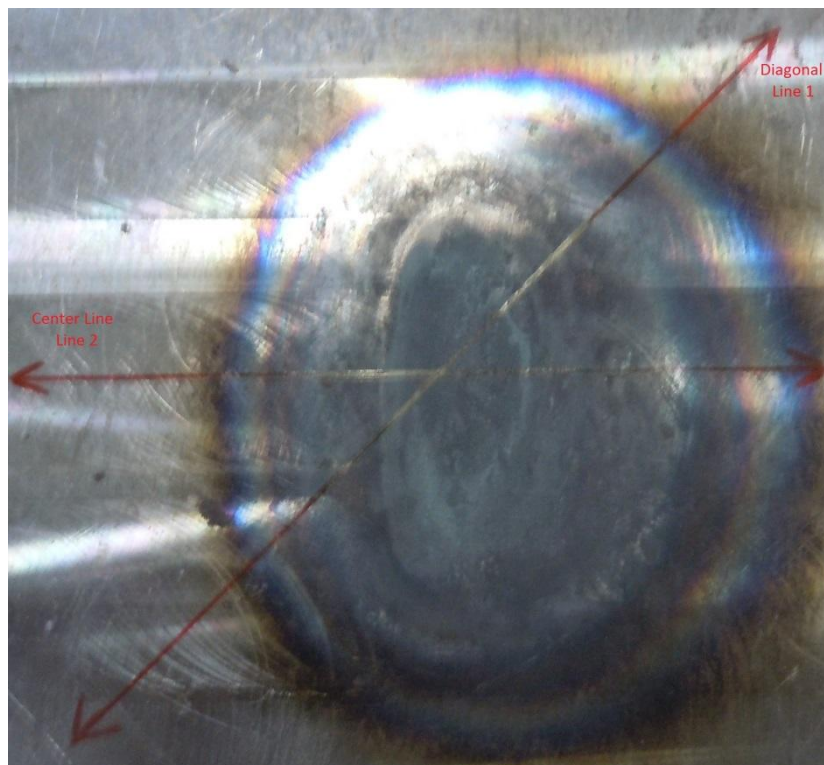
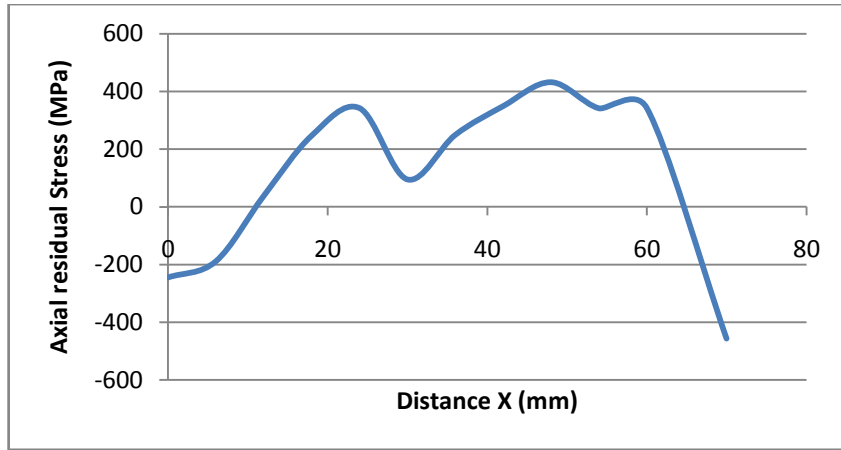
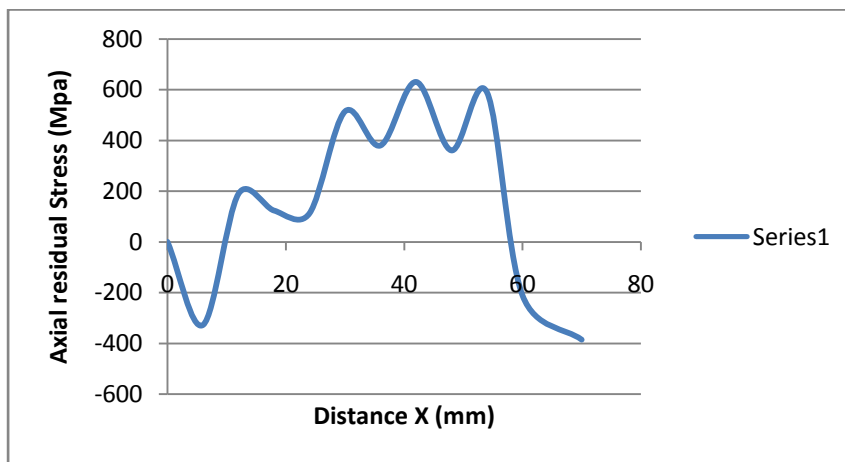


Figure 4.8: XRD Measurement of Residual stress axially and diagonally

The finite element results are in qualitative agreement while quantitatively the finite element model can't give reliable results.



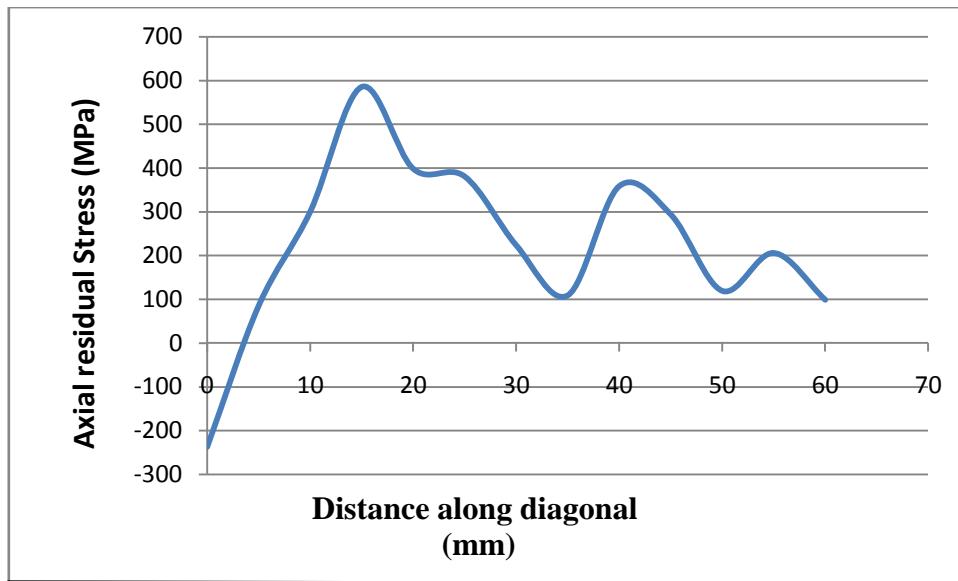
(a) Simulated Axial residual stress



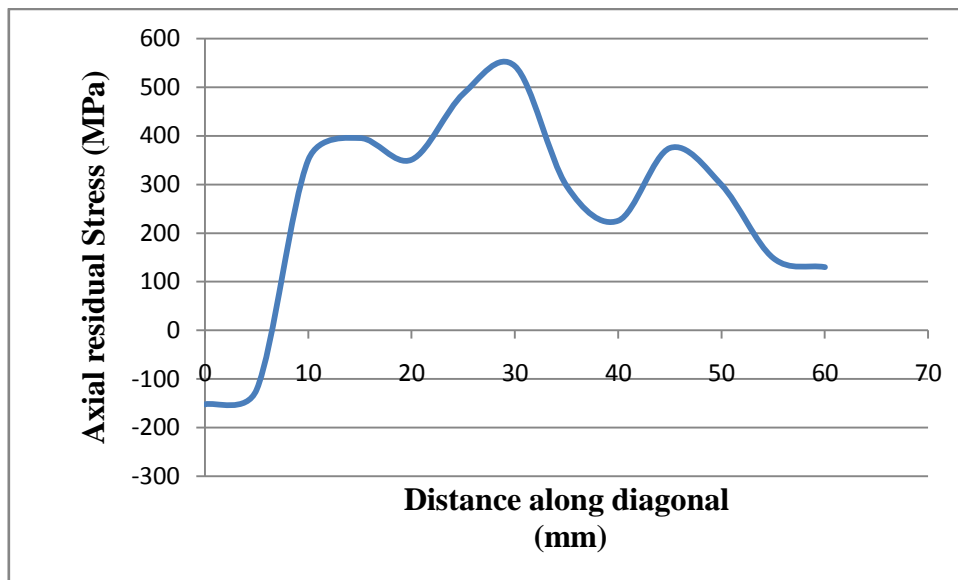
(b) Experimental Axial residual stress

Figure 4.9 : Comparison between experimental and simulated residual stress axially

The axial residual stresses along Line 2, is shown in Figure 4.9, on the back side of the base plate. It is very evident from the above plots that the peak axial stresses are found in areas of (X=30 & X= 40), while lower residual stresses exists at the deposition start side (X=60). This variation occurs due to the reheating effect of successive passes. When molten metal is deposited, high tensile stresses appears due to restraint thermal contraction but when next row is deposited the reheating relaxes the stress, therefore the areas which are reheated, give comparatively low residual stresses.



(a) Simulated residual stress along diagonal



(b) Experimental residual stress along diagonal

Figure 4.10 : Comparison between experimental and simulated residual stress diagonally

In the above comparison graphs see fig. 4.10., a good match was made between the simulated and experiment results. The stresses are measure along the diagonal line (Line 1).

Chapter 5

Conclusion and Future Scope

5.1 Conclusion

A 3-D finite element model is developed to predict the residual stresses associated with the single layer metal deposition employing modified heat source of twin wire welding for zig-zag path. The analysis is capable of predicting the temperature gradient and thermally induced stress distribution on the base plate as a result of the material deposition process. Finite element analysis is done using ANSYS Mechanical APDL and it is validated experimentally. Experimental validation is done using time twin robotic welding and the residual stress is measured using XRD residual stress measuring instrument. From the numerical and experimental results it is observed that, the temperature and residual stress are found to be high at the start point of the deposition path then it gradually reduces towards the end point, because the fore pass preheat the plate for the rear pass. The numerical results show marginal deviation in values with comparison to the experimental value. This might be because of the material model and heat source equations that are considered in FEA modelling.

The following conclusions can be made from the above simulation and experiment results

1. Residual stresses are caused due to the thermal gradient that is caused due to welding operation.
2. Temperature distribution and residual stresses at concerned locations are measured to verify the finite element model of weld-deposition based additive manufacturing. Experimental measurements are in agreement with simulated results with minimal deviation.
3. In the weld-deposition based additive manufacturing; the heat losses of component mainly include the heat conduction, the heat convection and the heat radiation. A thermal insulation between the fixture and the base plate can reduce the deviation between experiment and numerical results.

5.2 Future Scope

Many attempts have been made over numerical simulations and finite element analysis for predicting the residual stress caused due the thermal gradient caused in the work piece during weld based additive manufacturing. Although the developed model is able to satisfactorily predict the residual stresses, the elimination of assumptions assumed in the model can enhance its accuracy.

Therefore a complete 3D model is essential for the accurate determination of residual stresses and deformations; however a single layer deposition model and multi-pass welding in a butt joint were performed by many others in the past. A perfect three dimensional model is recommended when aim is to study the relative effect of different process parameters due to cyclic thermal loading. The ultimate aim of the project is to build a functionally gradient object or matrix through weld-deposition based additive manufacturing.

References

- [1] I. Rosen, David W Gibson and B. Stucker, “Additive manufacturing technologies: rapid prototyping to direct digital manufacturing”. New York, NY: Springer, 2010.
- [2] T. J. Gornet, K. . Davis, T. . Starr, and K. .Mulloy, “Proceedings of the solid freeform fabrication symposium characterization of selective laser sintering materials to determine process stability,” Univ. Tex. Austin Usa, 2002.
- [3] H.E. Beradsley, and R. Kovacevic, "New Rapid Prototyping Technique Based on 3D Welding," Proc. of the 31st CIRP International Seminar on Manufacturing Systems Berkeley, CA., 1998.
- [4] N. N. Rykalin, "Berechnung der Wärmevergänge beim Schweißen", VEB Verlag Technik, Berlin, 1957(Original: “Raschetye plovnykh protsessov prizrake”, Moscow, Mashgiz, 1951).
- [5] B. A. Boley and J. H. Weiner, Theory of thermal stresses. Mineola, NY: Dover Publications, 1997.
- [6] J. A. Goldak and M. Akhlaghi, *Computational Welding Mechanics*, Softcover reprint of hardcover 1st ed. 2005 edition. Springer, 2010.
- [7] Y. Ueda and T. Yamakawa, “Analysis of Thermal Elastic-Plastic Stress and Strain during Welding by Finite Element Method,” Transactions of the Japan Welding Society, vol. 2, no. 2, pp. 186–196, Sep. 1971.
- [8] H. D. Hibbitt and P. V. Marcal, “A numerical, thermo-mechanical model for the welding and subsequent loading of a fabricated structure,” Computers & Structures, vol. 3, no. 5, pp. 1145–1174, Sep. 1973.
- [9] L.-E. Lindgren, “Finite Element Modeling and Simulation of Welding Part 1: Increased Complexity,” Journal of Thermal Stresses, vol. 24, no. 2, pp. 141–192, 2001.
- [10] L. E. Lindgren, *Computational Welding Mechanics: Thermomechanical and Microstructural Simulations*, 1 edition. Cambridge, England; Boca Raton: CRC Press, 2007.
- [11] F. Kong and R. Kovacevic, “3D finite element modeling of the thermally induced residual stress in the hybrid laser/arc welding of lap joint,” J. Mater. Process. Technol., vol. 210, no. 6–7, pp. 941–950, Apr. 2010.
- [12] S. Feli, M. E. Aalami Aalegha, M. Foroutan, and E. Borzabadi Farahani, “Finite Element Simulation of Welding Sequences Effect on Residual Stresses in Multipass Butt-Welded Stainless Steel Pipes,” J. Press. Vessel Technol., vol. 134, no. 1, pp. 011209–011209, Dec. 2011.

- [13] D. Stamenković and I. Vasović, “Finite element analysis of residual stress in butt welding two similar plates,” *Sci. Tech. Rev.*, vol. 59, no. 1, pp. 57–60, 2009.
- [14] D. Gery, H. Long, and P. Maropoulos, “Effects of welding speed, energy input and heat source distribution on temperature variations in butt joint welding,” *J. Mater. Process. Technol.*, vol. 167, no. 2–3, pp. 393–401, Aug. 2005.
- [15] Y. Zhang and Y. K. Chou, “Three-dimensional finite element analysis simulations of the fused deposition modelling process,” *Proc. Inst. Mech. Eng. Part B J. Eng. Manuf.*, vol. 220, no. 10, pp. 1663–1671, 2006.
- [16] Amudala babu and Lakshmana kishore, “Finite element simulation of hybrid welding process for welding 304 austentic stainless steel plate,” *IJRET*, vol. 1, no. 3, pp. 401–410, Nov. 2012.
- [17] J. Goldak, A. Chakravarti, and M. Bibby, “A new finite element model for welding heat sources,” *Metall. Trans. B*, vol. 15, no. 2, pp. 299–305, Jun. 1984.
- [18] Ibiye Aseibichin Roberts, “Investigation of residual stresses in the Laser melting of metal powders in the additive layer manufacturing.” Sep-2012.
- [19] Kamran Shah, “Laser Direct Metal Deposition of dissimilar and functionally graded alloys,” PhD thesis, 2011.
- [20] U. N. Kempaiah and P. D. Sudersanan, “The effect of heat input & travel speed on the welding residual stress by finite element method,” *International Journal of Mechanical and Production Engineering Research and Development (IJMPERD)*, vol. 2, no. 4, pp. 43–50, 2012.
- [21] Rajalaxmi N. Mhetre and S.G. Jadhav, “Finite Element Analysis of welded Joints,” Mechanical Engineerng Dept., VJTI, Mumbai, India.
- [22] Hani Aziz Ameen, Khairia Salman Hassan, and MuwafaqMedi Salah, “Influence of the butt joint design of TIG welding on the thermal stresses,” *Eng. Tech. J.*, vol. 29, no. 14, pp. 2841–2849, 2011.
- [23] Daniel Berglund, Lars-Erik Lindgren and Andreas Lundbäck, “Three-dimensional finite element simulation of laser welded stainless steel plate,” proceedings of the 7th International conference on numerical methods in industrial forming processes - NUMIFORM 2001. ed./Ken-ichiro Mori. Lisse :Balkema Publishers, A.A. / Taylor & Francis The Netherlands, 2001. p. 1119-1124.
- [24] H. R. A. Lundbck, “Validation of three-dimensional finite element model for electron beam welding of Inconel 718,” *Science and Technology of Welding & Joining*, vol. 10, no. 6, pp. 717–724, 2005.

- [25] H. Zhao, G. Zhang, Z. Yin, and L. Wu, "Three-dimensional finite element analysis of thermal stress in single-pass multi-layer weld-based rapid prototyping," *Journal of Materials Processing Technology*, vol. 212, no. 1, pp. 276–285, Jan. 2012.
- [26] M. P. Mughal, H. Fawad, and R. Mufti, "Finite element prediction of thermal stresses and deformations in layered manufacturing of metallic parts," *Acta Mechanica*, vol. 183, no. 1–2, pp. 61–79, May 2006.
- [27] Q. G. Meng, H. Y. Fang, J. G. Yang, and S. D. Ji, "Analysis of temperature and stress field in Al alloy's twin wire welding," *Theoretical and Applied Fracture Mechanics*, vol. 44, no. 2, pp. 178–186, Nov. 2005.
- [28] www.fronius.com/
- [29] R. I. Karlsson and B. L. Josefson, "Three-Dimensional Finite Element Analysis of Temperatures and Stresses in a Single-Pass Butt-Welded Pipe," *J. Pressure Vessel Technol.*, vol. 112, no. 1, pp. 76–84, Feb. 1990.